Hepatitis C virus NS5A targets the nucleosome assembly protein NAP1L1 to control the innate cellular response

[1,4,#]Recep Emrah Çevik, [1,#]Mia Cesarec, [2]Ana Da Silva Filipe, [3]Danilo Licastro, [2]John McLauchlan and [1]Alessandro Marcello

[1]Molecular Virology Laboratory, International Centre for Genetic Engineering and Biotechnology (ICGEB), Trieste, Italy
[2]MRC-University of Glasgow Centre for Virus Research, Glasgow, United Kingdom
[3]CBM, Trieste, Italy
[4]Current address: The Scientific and Technological Research Council of Turkey, Ankara, Turkey.

[#]These authors contributed equally to this work.

Corresponding Author:

Alessandro Marcello, PhD
Head, Laboratory of Molecular Virology
International Centre for Genetic Engineering and Biotechnology (ICGEB)
Padriciano, 99
34149 Trieste, ITALY
tel: +39 040 375 7384 (office) 7385 (lab)
fax: +39 040 226555
http://www.icgeb.org/molecular-virology.html

Abstract

Hepatitis C virus (HCV) is a single-stranded positive-sense RNA hepatotropic virus. Despite cellular defenses, HCV is able to replicate in hepatocytes and to establish a chronic infection that could lead to severe complications and hepatocellular carcinoma. An important player in subverting the host response to HCV infection is the viral non-structural protein NS5A that, in addition to its role in replication and assembly, targets several pathways involved in the cellular response to viral infection. Several unbiased screens identified the nucleosome-assembly protein 1-like 1 (NAP1L1) as an interaction partner of HCV NS5A. Here we confirm this interaction and map it to the C-terminus of NS5A of both genotype 1 and 2. NS5A sequesters NAP1L1 in the cytoplasm blocking its nuclear translocation. However, only NS5A from genotype 2 HCV, but not from genotype 1, targets NAP1L1 for proteosomal-mediated degradation. NAP1L1 is a nuclear chaperone involved in chromatin remodeling and we demonstrate the NAP1L1-dependent regulation of specific pathways involved in cellular responses to viral infection and cell survival. Among those we show that lack of NAP1L1 leads to a decrease of RELA protein levels and a strong defect of IRF3 TBK1/IKKε-mediated phosphorylation leading to inefficient RIG-I and TLR3 responses. Hence, HCV is able to modulate the host cell environment by targeting NAP1L1 through NS5A.

Importance

Viruses have evolved to replicate and to overcome antiviral countermeasures of the infected cell. The hepatitis C virus is capable of establishing a life-long chronic infection in the liver, which could develop into cirrhosis and cancer. Chronic viruses are particularly able to interfere with the cellular antiviral pathways by several different mechanisms. In this study we identify a novel cellular target of the viral non-structural protein NS5A and demonstrate its role in antiviral signaling. This factor, called nucleosome-assembly protein like 1 (NAP1L1), is a nuclear chaperone involved in the remodeling of chromatin during transcription. When depleted, specific signaling pathways leading to antiviral effectors are affected. Therefore, we provide both evidence for a novel strategy of virus evasion from cellular immunity and a novel role for a cellular protein, which has not been described to date.

Keywords: HCV; NAP1L1; innate immunity; IRF3, NF-kB; RIG-I; TLR3

Introduction

HCV is a member of the *Flaviviridae* family, genus *Hepacivirus*, with a single-stranded positive-polarity RNA genome of approximately 9.6 kb (1). Seven viral genotypes (1 to 7) have been identified with important differences in geographical distribution, pathogenesis and response to treatment (2). The HCV life cycle is entirely cytoplasmic and involves entry, uncoating and translation of the viral RNA to a polyprotein that is processed by proteolysis into 3 structural (Core, E1 and E2) and 7 non-structural proteins (p7, NS2, NS3, NS4A, NS4B, NS5A, NS5B). Viral RNA translation, replication and subsequent steps of particle assembly and release takes place associated with remodelled intracellular membranes and lipid droplets (LD) (3-5). Non-structural proteins are required for RNA replication, with NS3-NS4A being the helicase/proteinase and NS5B being the viral RNA-dependent RNA polymerase. In addition, HCV non-structural proteins have also been implicated in perturbing cell signalling and mediating immune evasion. Among them, NS5A has been implicated in subverting several cellular pathways and as a candidate viral oncogene.

NS5A is a 447aa (gt-2a) phosphoprotein that is found associated to ER membranes through an N-terminal amphipathic helix (aa 1-27). The rest of the polypeptide is hydrophilic and consists of a large amino-terminal domain I followed by two smaller, more variable domains II and III. Domains I and II are essential for viral genome replication while domain III is dispensable for genome replication, but is required for viral particle assembly via interaction with Core (6-8). A cluster of phosphorylated Serine residues at position 452/454/457 (strain JFH1 gt-2a) at the very C-terminal end of NS5A is responsible for this interaction. In addition to a direct role in HCV genome replication and assembly, NS5A makes an important contribution to modulating the host cell environment. NS5A is a promiscuous protein and interacts with several host factors thus affecting different signalling pathways that control cell cycle, apoptosis and the interferon response to viral infection (reviewed in: (9, 10)).

Chronic infection with HCV is a major risk factor for the development of hepatocellular carcinoma (HCC) (11). The leading hypothesis is that malignant transformation of hepatocytes occurs through increased liver cell

turnover induced by chronic liver injury and regeneration, in a context of inflammation and oxidative DNA damage. However, increasing experimental evidence suggests that HCV might also contribute to malignant transformation of hepatocytes through the direct action of viral proteins on cellular transformation pathways (12). Liver-specific expression in transgenic mice of the full viral polyprotein (Core to NS5B) at low levels, comparable to those found in patients, has been shown to induce HCC without inflammation (13). Mice transgenic for NS5A alone may also develop liver cancer, depending on the genetic background of the mice (14, 15). Furthermore, expression of NS5A in NIH3T3 fibroblasts promoted anchorage-independent growth and tumour formation in nude mice (16, 17). These data support a direct role of HCV proteins, and NS5A in particular, in the development of HCC.

In a recent attempt to identify host factors that associate with a number of innate immune-modulating viral proteins, Pichlmair et al. screened novel proteins that interact with HCV NS5A (18). Careful inspection of the data led to the unexpected observation that NS5A interacted with the human nucleosome assembly protein-like 1 (NAP1L1 or hNAP1). The interaction of NS5A with NAP1L1, or with the highly homologous NAP1L4, was independently identified in at least another three independent reports (19-21).

NAP1L1 was originally identified in HeLa cells as the human homolog of the yeast nucleosome assembly protein 1 (NAP-1) (22). NAP1L1 is a 391aa polypeptide characterized by nuclear import/export sequences and histone and protein binding domains (23). NAP1L1 is a chaperone and nucleo-cytoplasmic shuttling factor that facilitates the delivery and incorporation of two histone H2A-H2B dimers to complete the nucleosome (reviewed in (24-26)). NAP1L1 has been involved in the regulation of transcription, cell-cycle progression, incorporation and exchange of histone variants and promotion of nucleosome sliding. In addition, NAP1L1 has been shown to interact with several host and viral factors including the coactivator p300 and E2 of papillomaviruses (27-29). NAP1L1 interacts with the human immunodeficiency virus type 1 (HIV-1) Tat transactivator and enhances HIV-1 trans-activation (30, 31). NAP1L1 family proteins are localized in the cytoplasm, but inhibition of nuclear export results in their accumulation in the nuclei indicating a shuttling activity that has been implicated also in the

delivery of histones to the nucleus as part of their chaperoning activity. NAP1L1 has been involved in the process of nucleosome depletion during embryonic stem cell differentiation (32). Knockdown of NAP1L1 enhanced the differentiation of iPSC into functional cardiomyocytes (33). NAP1L1 expression has also been shown to be elevated in several cancers (34-36).

In this work we confirm the interaction of NS5A with NAP1L1 and its co-localization in the cytoplasm of cells replicating HCV. The interaction could be mapped to the carboxy-terminus of domain III of NS5A, which is shared among all HCV genotypes. However, only NS5A from genotype 2, but not from genotype 1, targets NAP1L1 for proteosomal-mediated degradation. RNAseq analysis of NAP1L1-depleted cells shows dis-regulation of a number of genes from pathways of innate immunity and cell survival. Among those, we show that depletion of NAP1L1 leads to the down-modulation of NF-κB and to a strong down-regulation of IRF3 phosphorylation mediated by the kinase TBK1/IKKε. Both the RIG-I and TLR3 pathways were affected by NAP1L1 depletion. We conclude that HCV is able to modulate the host cell environment by targeting NAP1L1 through NS5A. We believe this may represent a novel strategy deployed by HCV to evade from cellular antiviral responses and possibly to maintain a chronic infection thus contributing to the development of HCC.

Results

HCV NS5A binds NAP1L1

In independent reports, the non-structural protein 5A (NS5A) from the human hepatitis C virus (HCV) has been repeatedly found to interact with the nucleosome assembly protein NAP1L1 (18-21). However, such reports didn't map the interaction or conducted additional functional studies. To confirm the interaction we generated a full-length flag-tagged f-NS5A (N-terminus) derived from JFH1 genotype 2a (gt2a). Co-transfection of f-NS5A with HA-NAP1L1 in HEK 293T cells followed by anti-flag affinity chromatography resulted in the detection of HA-NAP1L1 (Figure 1A). As a positive control for the interaction we used the human immunodeficiency virus Tat protein, which has been previously described to bind NAP1L1 (30, 31). To study the interaction of NS5A with NAP1L1 at the endogenous levels we took advantage of the JFH1 subgenomic replicon (SGR-JFH1/Luc), which efficiently replicates in hepatocytes. As shown in Figure 1B, the interaction was preserved, albeit with a very low efficiency of immunoprecipitation, which could be explained by an effect of NS5A on the stability of the protein (see below). Furthermore, extensive colocalization of the two proteins was observed in the cytoplasm (Figure 1C). Interestingly, the extent of the co-localization increased from approximately 10% of NS5A expressing cells at 48 hpe to more than 70% at 72 hpe (not shown). We repeated the experiment with a sub-genomic replicon that expresses also HCV Core (Luc-JFH1ΔE1/E2) (37). In this case NS5A drives the localization of NAP1L1 to subcellular locations reminiscent of lipid droplets (Figure 1C, lower panels). However, the interaction between NS5A and Core was not required for the NS5A to bind NAP1L1, as demonstrated in the experiments conducted in the absence of Core (Figure 1C top panels and Figure 1AB).

HCV NS5A from gt2 mediates NAP1L1 proteosomal degradation

In order to investigate if the interaction with NAP1L1 was shared by NS5A from other HCV genotypes we performed an IP with genotype 1 (gt1) Con1- and H77-derived proteins. Surprisingly, NS5A from gt1 isolates was able to IP higher levels of NAP1L1 compared to JFH1 NS5A (Figure 2A).

Furthermore, co-transfection of HA-NAP1L1 with increasing amounts of JFH1 NS5A (gt2) resulted in a decrease of NAP1L1 levels, while Con1 NS5A (gt1) did not (Figure 2B). Hence, NS5A from JFH1 (gt2), but not those from Con1 or H77 (gt1), resulted in the degradation of NAP1L1. Treatment with the inhibitor MG132 partially rescued the JFH1 NS5A degradation of NAP1L1 indicating proteasome involvement (Figure 2C). Finally, cycloheximide treatment of SGR-JFH1/Luc transfected cells showed a progressive decrease of endogenous NAP1L1, although less efficiently than transfecting NS5A alone (Figure 2B), possibly related to the different levels of NS5A expression in the two experimental conditions. Degradation of NS5A could be rescued by MG132, further highlighting the targeting of NAP1L1 for proteosomal-mediated degradation also at physiological levels during HCV replication (Figure 2D). The major difference between JFH1-derived NS5A and those of the other HCV genotypes resides in a 20 amino acids insertion at the carboxy-terminal end of the protein (Figure 2E), which also accounts for the differences of molecular weight observed (Figure 2A).

We conclude that NAP1L1 binding is shared among NS5A derived from g1 and gt2 genotypes, but gt2 NS5A has the additional feature of being able to target NAP1L1 for proteosomal-mediated degradation.

The carboxy-terminus of NS5A is required for NAP1L1 binding

In order to map the interaction, NS5A from JFH1 was divided in three domains: Domain I (D1, nt. 2003-2189), Domain II (D2, nt. 2226-2314), Domain III (D3, nt. 2328-2442) all linked in various combinations to the N-terminal amphipatic helix for membrane tethering, and flag-tagged at the N-terminus (Figure 3A). As shown in Figure 3B, only constructs maintaining D3 could interact with NAP1L1. Therefore, NS5A was further truncated from the C-terminus to generate proteins with progressive deletions. With this approach we found that deletions starting from the acidic motif 458-EEDD-461 (AH-D3.5 in Figure 3C) completely abolished the interaction with NAP1L1. Since the acidic motif is a perfect consensus for casein kinase 2 mediated Serine phosphorylation (CK2: S-D/E-X-E/D) we reasoned that NAP1L1 interacts with the C-terminal cluster of Serines already implicated in the interaction with HCV Core (6-8). To this end, we tested both the delB deletion

mutant of aa 2419-2433 (residues are numbered according to the positions within the original JFH1 polyprotein corresponding to aa 443-457 of NS5A) (7) and the triple mutant of cluster 3B (CL3B/SA or m2) (corresponding to S2428/2430/2433A, aa S452/454/457A of NS5A) (6). Co-IP analysis showed loss of interaction for both mutants (Figure 3D) further suggesting that these residues are crucial for NAP1L1 interaction. To further demonstrate that the co-localization requires the interaction of NS5A with NAP1L1 through the C-terminal Serine-rich region we exploited two sub-genomic constructs SGR-delB, and SGR-m2 (6, 7). NS5A from both constructs localized in clusters in the cytoplasm, like the wild-type replicon, but did not co-localize with NAP1L1, which remained diffused in the cytoplasm (Figure 3E). We conclude that NAP1L1 binds to the same cluster of serine residues at the carboxy-terminus of NS5A as the HCV core protein.

NAP1L1 is not required for HCV replication and infectivity in Huh7 cells

In order to assess the potential role of NAP1L1 in HCV replication we overexpressed the EYFP-tagged version of NAP1L1 in Huh7-Lunet cells by lentiviral vector (LV) transduction. NAP1L1-EYFP had the expected cytoplasmic localization and co-localized with NS5A when cells were transfected with SGR-JFH1 RNA (Figure 4A). However, there was no difference between cells overexpressing NAP1L1-EYFP or EYFP alone in the levels of luciferase from SGR-JFH/Luc, which is a measure of HCV genome replication (Figure 4B). Next, we efficiently depleted NAP1L1 by lentivectors delivering a specific shRNA (Figure 4C). Again, Huh7-Lunet cells replicated SGR-JFH/Luc in conditions of NAP1L1 depletion as well as in mock conditions (Figure 4D). To further confirm these results, we introduced full-length genomic HCV JFH1 RNA into Huh7-lunet cells, which had been treated with shRNA as above. Cell culture supernatants at the indicated time points were used to infect naïve Huh7.5 cells to measure infectivity. As shown in Figure 4E, also HCV infectivity was not affected by NAP1L1 depletion in Huh7-lunet cells. Finally, we investigated the replication of HCV SGR-JFH/luc carrying the m2 mutation of NS5A. As shown in Figure 4F, wild type and m2 replicons replicated equally well in Huh7-Lunet cells, compared to the non-replicative control mutated in the polymerase NS5B GND.

We took the inverse approach to investigate the effect of NS5A on NAP1L1 activity. In physiological conditions in cell culture NAP1L1 is found predominantly in the cytoplasm (Figure 1C). However, incubation of cells with the nuclear export inhibitor Leptomycin B (LMB) results in the accumulation of NAP1L1 in the nucleus (Figure 5A) (31). Therefore, we transfected cells with SGR-JFH1 and its mutant m2 and monitored the localization of endogenous NAP1L1 in the nucleus. As shown in Figure 5A & 5B, SGR-driven NS5A, but not the m2 mutant, significantly inhibited nuclear localization of NAP1L1. To further analyze this phenotype in the context of HCV gt1 we engineered the corresponding m2 mutations also in Con1-derived NS5A (see Figure 2E for an alignment of the carboxyterminus of NS5A from the different genotypes). As shown in Figure 5C, Con1-derived NS5A m2 lost the ability to interact with NAP1L1 as expected. Interestingly, both JFH1 and Con1-derived NS5A equally inhibited nuclear translocation of NAP1L1 (Figure 5D & 5E).

We conclude that NAP1L1 is not directly involved in HCV replication and infectivity, but NS5A from both genotypes affect NAP1L1 nuclear localization, possibly by sequestering NAP1L1 in the cytoplasm. Hence, we set to investigate the nuclear activity of NAP1L1.

Transcriptome analysis of NAP1L1-depleted cells

NAP1L1 is a nucleosome chaperone involved in several nuclear processes including transcription. Genome-wide analysis of yNAP1-deleted *Saccharomyces cerevisiae* showed that about 10% of all yeast open reading frames changed the transcription levels more than 2-fold (38). To investigate the transcriptome of hepatocytes we depleted NAP1L1 with shNAP1L1 (Figure 4C). Differential analysis of the shNAP1L1 trascriptome versus cells transduced with the control shRNA (shCTRL) showed significant up-regulation of 144 genes (fold change ≥ 2) and down-regulation of 358 genes (fold change ≤ 2) with a false discovery rate of less than 0.05 (data derived from the most stringent DESEQ2 statistical analysis of Supplementary Table 1, which also shows the EDGR statistical analysis of the same data for comparison). These numbers correspond to approximately 1% of the total reads of the analysis (46623 reads) suggesting a good degree of specificity for the genes regulated by NAP1L1. To validate the sequencing data we re-

tested a number of modulated genes by RT PCR as shown in Figure 6A. Ingenuity pathway analysis of down-regulated genes indicated that top canonical pathways involved in cancer and signaling were mostly affected (Supplementary Table 1). Interestingly, we also noticed down-modulation of interferon-stimulated genes (ISG) such as IFITM3, GBP2 and UBD as well as genes involved in interferon (IFN) transcriptional activation such as RELA (p65 subunit of NF-κB), c-Jun and GEF2 (39, 40). To investigate if the expression of the NAP1L1 target genes is reduced in HCV infected cells we conducted a meta-analysis of published data obtained in a similar setting (41). We found an overlap of 40 genes between the two analysis with 5 up-regulated genes, 27 down-regulated genes and 8 genes showing opposed regulation. Interestingly, among the overlapping down-regulated genes we found again genes implicated in innate immunity regulation such as RELB, c-Jun, and GEF2 (Supplementary Table 2). We also compared Huh7 cells stably replicating SGR JFH-1 with the homologous cured cells for the expression of some NAP1L1 regulated genes (not shown). We found that two significantly down-regulated genes in the context of NAP1L1 depletion such as GEF2 and IFTM1 where also down-regulated in conditions that favor HCV replication. However, other genes were not affected (CFL2 and HEPACAM2) or showed opposite regulation (UBD).

In order to explore the impact of NAP1L1 depletion on the interferon response pathway we explored IFNα-mediated induction of IFITM3, GBP2 and UBD (as well as IFIT1, IFIT3, OASL, IL8 and CXCL11, not shown). We found that these genes were not impaired in their IFN-dependent induction by NAP1L1 depletion, ruling out a specific role for NAP1L1 in ISG transcriptional activation (Figure 6B). Finally, in order to assess the effect of NAP1L1 depletion on the induction of IFNβ we needed a different cell line from Huh7-derived cells. To this end we used U2OS cells that maintain an intact IFN-signaling pathway following poly(I:C) transfection, compared to cells more permissive to HCV such as Huh7-Lunet or Huh7.5 (Figure 6C) (42, 43). However, as shown in Figure 5D and 5E, the IFNβ response to poly(I:C) transfection in U2OS cells was completely obliterated in the absence of NAP1L1, both at the mRNA and protein level. Similar results were also obtained in the context of vesicular stomatitis virus infection (not shown).

These data indicate that NAP1L1 is involved in regulating pathways that lead to interferon induction.

Involvement of NAP1L1 in the induction of IFN

Pattern recognition receptors (PRR) like RIG-I/MDA5 and TLR3 respond to viral RNA agonists as well as to poly(I:C) by activating transcription factors such as NF-κB and IRF3. We observed previously that the NF-κB subunit RELA mRNA levels were reduced in the context of NAP1L1 depletion (Figure 6A) and we confirmed this also at the protein level (Figure 7A and quantification Figure 7B). Following activation, RELA translocates into the nucleus as a phosphorylated protein. As shown in Figure 7A (quantification in Figure 7C), phosphorylation of RELA occurs 1-4 hours post polyI:C induction. In conditions of NAP1L1 depletion, albeit in conditions of reduced RELA protein content, phosphorylation occurs normally up to 4 hours post-treatment, when a slight decrease was consistently observed (Figure 7A and quantification in Figure 7C). Nuclear translocation of RELA showed a significant decrease in the context of NAP1L1 depletion following polyI:C induction (Figure 7D and 7E). At variance with RELA, IRF3 protein levels were not changed by NAP1L1 depletion (Figure 7A). However, IRF3 phosphorylation was profoundly affected (Figure 7A and quantification in Figure 7C) as well as IRF3 nuclear translocation (Figure 7F and 7G). Finally we wished to recapitulate the phenotype of NAP1L1 depletion using HCV NS5A. Wild-type NS5A inhibits TBK1-mediated activation of the IFN response (Figure 7H), but the activity was rescued by the NS5A mutant that cannot bind NAP1L1. These results suggest that NAP1L1 depletion regulates the innate immune response by down-modulating RELA protein levels and by inhibiting IRF3 phosphorylation.

Molecular basis of NAP1L1 depletion on IRF3 phosphorylation

IRF3 phosphorylation is the consequence of a complex series of molecular events (see diagram in Figure 8A). PRRs such as RIG-I recognize the RNA agonist in the cytoplasm and bind the adaptor protein IPS-1/MAVS to trigger the downstream kinases TBK1/IKKε, which then phosphorylate IRF3. TLR3 instead recognizes the RNA agonist within endosomes and signals through

the adaptor TRIF to induce IRF3 phosphorylation. Since NAP1L1 depletion could affect each of these steps, we proceeded to dissect the whole signaling pathway. First, we took advantage of the constitutively active phosphomimetic IRF3-5D (44). Consistent with our interpretation, induction of IFNβ by IRF3-5D was not affected by NAP1L1 depletion (Figures 8B & 8C). Conversely, depletion of NAP1L1 resulted in the inhibition of each step of the RIG-I pathway, from MAVS down to TBK1/IKKε kinases. With a similar approach, we could demonstrate that the TLR3 adaptor protein TRIF activity is inhibited by NAP1L1 depletion (Figure 9A). To further investigate this pathway we reconstituted the TLR3 pathway in Huh7-lunet cells depleted for NAP1L1 (Figures 9B & 9C). Stimulation with exogenous p(I:C) induced high levels of the ISG IFIT1 (interferon induced protein with tetratricopeptide repeats 1), which was severely affected by NAP1L1 depletion (Figure 9D). We conclude that NAP1L1 controls both arms of innate sensing at the IRF3 crossroad.

Discussion

The co-evolution of viruses with their host results in a number of defense strategies and countermeasures. Particularly for chronic infections, where the virus persists for long periods of time, a delicate equilibrium is established to permit limited virus replication in the context of a permissive cellular environment. HCV is highly successful at establishing a chronic infection, with about 80% of patients that become chronically infected. In this work we describe several lines of evidence that identify NAP1L1 as a key cellular effector of innate sensing and propose a novel mechanism that the virus deploys to subvert innate immunity in infected hepatocytes.

First, we confirmed that NAP1L1 is a *bona fide* interactor of NS5A. These data are in support of a series of independent observations from other groups that indicated NAP1L1 and/or NAP1L4 as binding partners for NS5A, but failed to identify a functional role (18-21). We mapped the interaction at the extreme carboxy-terminus of NS5A, in a conserved motif encompassing three Serine residues that have been implicated in the interaction of NS5A with Core, which is essential for virus assembly, but dispensable for HCV genome replication (Figure 4F) (6-8). Interestingly, NAP1L1 has also been identified as a binding partner of Core in the same proteomic screenings that identified it as a binding partner of NS5A (18, 21). Indeed, in the presence of Core, we could visualize NAP1L1 on the surface of lipid droplets together with NS5A and Core. However, interaction with Core appears not to be essential for NAP1L1 and NS5A interaction, since experiments conducted in the absence of Core showed efficient interaction and co-localization. Therefore, Core and NAP1L1 bind independently the same region of NS5A. Unfortunately, mutagenesis of the binding motif in NS5A results in the disruption of both Core and NAP1L1 interactions and in a defect in assembly for viruses generated with these mutations, thus precluding their use unless these two interactions are uncoupled, if at all possible.

Next we questioned the functional role of the interaction. We discovered that NS5A from genotype 2 was able to bind and degrade NAP1L1 through a proteosomal-dependent mechanism. NS5A from genotype 1 was also able to bind efficiently, but unable to degrade NAP1L1. Furthermore, wild-type NS5A

421 from both genotypes, but not the mutated version defective for NAP1L1
422 binding, inhibited the nuclear re-localization of NAP1L1. It is well established
423 that acutely infected patients respond well to IFN therapy while in chronically
424 infected ones the response to IFN is variable and depends on the viral
425 genotype (39, 45). Patients infected with HCV genotype 2 and 3 show a better
426 response compared to genotypes 1 and 4, which correlates with higher levels
427 hepatic ISG expression in HCV genotype 1 and 4 infected patient liver before
428 therapy (46-49). The ability of different genotypes to subvert the innate
429 response has been ascribed to the genetic variability of NS3 and NS5A, which
430 could affect their known activities in targeting innate immunity effectors such
431 as MAVS (NS3) or PKR and possibly NAP1L1 (NS5A). For example, the
432 levels of MAVS cleavage *in vivo* showed a positive correlation with the
433 decrease of the interferon response (50). In that report, HCV genotypes 2 and
434 3 were more efficient than genotype 1 and 4 in MAVS cleavage and blockage
435 of the endogenous IFN system, which determines the response to the
436 treatment with pegylated IFN and ribavirin. Therefore we could speculate that
437 also the differential ability of NS5A from genotype 1 (binding of NAP1L1) and
438 2 (binding and degradation of NAP1L1) contributes to the observed responses
439 following IFN treatment. However, the interaction of NS5A and NAP1L1
440 appears functionally dominant over JFH1 dependent degradation. In fact,
441 NS5A from the two genotypes were observed to be equally efficient in
442 blocking NAP1L1 translocation into the nucleus (Figure 5C and D).
443 Depletion of NAP1L1 by shRNA, which recapitulates NS5A-mediated
444 inhibition, resulted in the modulation of several genes at the transcription
445 level. In particular, we noticed down-modulation of interferon-stimulated genes
446 (ISG), such as GBP2, IFITM3 and UBD, and genes involved in the
447 transcriptional activation of IFNβ such as RELA, the p65 subunit of NFκB.
448 Indeed, depletion of NAP1L1 strongly affected polyI:C mediated induction of
449 IFNβ, while no effect was observed for IFNβ induction of ISGs. These findings
450 restrict the functional role of NAP1L1 on HCV to the modulation of the innate
451 sensing of the virus in infected cells. It is worthwhile noting that the latter
452 experiments were conducted in U2OS cells, which are competent for the
453 interferon response (43). Huh7-derived cell lines adapted for HCV growth are
454 instead defective for the sensing of HCV replication (see Figure 5C) (42, 43).

Hence, NS5A control of NAP1L1 results in the inhibition of the cellular innate response pathway leading to IFNβ transcription, which is appreciable only in cells that maintain this pathway active. This observation clearly explains why we failed to observe any effect of NAP1L1 overexpression or depletion on HCV replication and infectivity in Huh7 derived cells.

HCV infection triggers a number of innate immune pathways (39). The 5'-ppp and the poly U/UC sequence of viral RNA are potent activators of RIG-I signaling through MAVS/IPS-1 leading to the activation of the transcription factors IRF3 and NF-κB, which in turn drive transcription of IFNβ. HCV infection is also monitored in the host by the Toll-like receptors (TLRs). Viral RNA activates TLR3 and signals are transduced through the TIR-domain containing adapter-inducing IFNβ (TRIF) leading to activation of the transcription factors IRF3 and NFκB for the induction of innate immunity (51, 52). Another recently described sensor protein for HCV is the antiviral protein kinase R (PKR). Kinase-independent PKR signaling activates specific ISGs and IFNβ early during HCV infection (53). This signaling induces protein–protein interactions between PKR and MAVS, which have been previously described as a signaling adaptor protein also for PKR (54-56). Interestingly, all these pathways converge on the activation of transcription factors NFκB and/or IRF3. We found that depletion of NAP1L1 not only results in a significant reduction of the mRNA and protein levels of NFκB, but also severely impairs IRF3 phosphorylation. Furthermore, nuclear translocation of both NFκB and IRF3 following polyI:C stimulation of RIG-I is reduced when NAP1L1 is depleted. Therefore, NAP1L1 affects a step leading to IRF3 phosphorylation, a conclusion that is further substantiated by an experiment where IFNβ expression induced by a constitutively active phosphorylated form of IRF3 (IRF3-5D) remains unaffected by NAP1L1 depletion, which rules out inhibitory effects downstream of IRF3 phosphorylation. In order to understand at which step NAP1L1 depletion was inhibiting the pathway upstream of IRF3 we proceeded to dissect the major RIG-I dependent axis leading to IFNβ expression. We could consistently observe that depletion of NAP1L1 reduces INFβ expression induced by activated RIG-I, MAVS, TBK1 and IKKε. Hence, we can hypothesize that NAP1L1 depletion affects the RIG-I pathway at the level of TBK1/IKKε phosphorylation of IRF3. As mentioned above, at this step

converge all three pathways of IFNβ activation by HCV: RIG-I, TLR3 and PKR. Indeed, the TLR3 pathway was also inhibited by NAP1L1 depletion. Finally, to demonstrate that NS5A targeting of NAP1L1 is sufficient to inhibit this phosphorylation step we show that wild type NS5A, but not NS5A mutants defective for NAP1L1 binding, are able to inhibit IFNβ induction by TBK1.

The master viral regulator of the HCV immune evasion program is the HCV NS3/4A protease. To regulate innate immune signaling, NS3/4A utilizes its protease domain to cleave key innate immune signaling adaptor proteins such as MAVS (57-60) and TRIF (61, 62). However, hepatitis A virus, a hepatotropic virus, which does not usually become chronic, encodes a protease that also cleaves MAVS (63). Thus, MAVS/TRIF cleavage is probably necessary but not sufficient for viral chronicity. HCV also regulates PKR activity during viral infection. HCV has several PKR-inactivation strategies that probably contribute to viral persistence in addition to NS3-NS4A cleavage of MAVS, which depend on the activity of NS5A and E2 (64-66). In this work we add another mechanism that could be deployed by HCV to subvert the host response to infection. We could not fully recapitulate the functional role of NAP1L1 in the infectious HCV life cycle due to a number of limitations of our experimental tools. First, mutations in NS5A that abolish NAP1L1 binding are not compatible with a fully infectious virus (6-8). Second, Huh7-derived cells that support HCV replication are impaired in the interferon response (Figure 6C). Third, Infection with full-length HCV would lead to several additional mechanisms of inhibition of the interferon response in addition to the NS5A/NAP1L1 axis, such as NS3/4A targeting MAVS and TRIF or NS2 inhibiting TBK/IKKε (39, 67). However, notwithstanding the limitations outlined above, we could clearly identify NAP1L1 as a target for HCV NS5A and define its novel role in the innate response. To note, a very recent report confirmed the interaction of HCV NS5A with NAP1L1 and showed some effect of NAP1L1 depletion on viral replication in the context of cells stably harboring a SGR HCV (68). It is possible that chronically replicating HCV is somehow more sensitive to NAP1L1 depletion.

NAP1L1 is a cytoplasmic protein unless stimulated to translocate into the nucleus. Therefore we initially hypothesized a direct participation of NAP1L1 in the TBK1/IKKε kinase complex that phosphorylates IRF3. However, we

failed to immunoprecipitate NAP1L1 together with TBK1 and IKKε (not shown). Most probably, the activity of NAP1L1 is at the transcriptional level instead, as we observed for the down-modulation of NFκB. NAP1L1 depletion and/or sequestration in the cytoplasm would result in the decrease of an as yet unknown cellular factor that promotes TBK1/IKKε phosphorylation of IRF3. Targeting general transcription factors to subvert innate sensing is not unusual. Several examples of viral proteins that target host cell transcription have been described. NSs from La Crosse encephalitis virus acts downstream of IRF3 by specifically inhibiting RNA polymerase II (RNAPII) mediated transcription by proteasomal degradation of the RBP1 subunit (69). Other Bunyaviruses interfere with RNAPII CTD Ser2 phosphorylation or target TFIIH (70-72). The NS1 of influenza A H3N2 subtype mimics a histone tail and suppresses hPAF1C-mediated transcriptional elongation of a subset of inducible genes involved in the antiviral response (73). Therefore, targeting transcription appears a generalized strategy to fine-tune transcriptional programs triggered by infection, which puts the cell in the optimal state to overcome the invaders' attack. HCV makes no exception and we demonstrate here that by targeting NAP1L1, it is able to control a subset of host genes, including key components of the antiviral innate sensing. It will be important to investigate at the transcriptional level the mechanism of action of NAP1L1 and to identify the factor(s) involved in TBK1/IKKε IRF3 phosphorylation that are down-modulated when NAP1L1 is depleted.

Materials and Methods

Cells and viruses

The human hepatocarcinoma Huh7 cell line, its derivative Huh7-lunet kindly provided by Ralf Bartenschlager (University of Heidelberg, Germany) (74), the HEK293T cell line and the osteosarcoma cell line U2OS were cultured in Dulbecco's modified Eagle's medium (DMEM) supplemented with 10% fetal bovine serum (FBS) and antibiotics. Cell cultures were maintained at 37 °C under 5% CO_2. Cells were routinely tested for mycoplasma contamination.

In vitro transcribed JFH1 RNA was introduced into Huh7-lunet cells by electroporation as described (75). The supernatants from cells electroporated with JFH1 RNA were removed at required time points and used to infect monolayers of naive Huh7.5 cells. Infected cells were detected at three days post-inoculation by indirect immunofluorescence using a polyclonal NS5A antiserum. The tissue culture 50% infectious dose ($TCID_{50}$) was determined by limiting dilution assay (76).

IFNα was obtained from the Biotechnology Development Group of the ICGEB.

Plasmids

Plasmid pJFH1 was provided by T. Wakita (77). Plasmids encoding SGR-JFH1/Luc and the non-replicating control SGR-JFH1/Luc-GND were described previously (78). Plasmid pFKLuc-JFH/ΔE1-E2 was provided by R. Bartenschlager (37), plasmid SGR-JFH/m2 was provided by T. Masaki (6) and plasmid SGR-JFH1/delB by T. Tellinghuisen (7). The pHA-NAP1L1 and pNAP1L1-EYFP expression vectors were described previously (30, 31). pFLAG CMV-2 (Sigma-Aldrich) was used as backbone for all NS5A constructs. Flag tagged NS5A from HCV JFH1, Con1 and H77 were cloned by PCR of the corresponding HCV genotypes. Mutagenesis of NS5A (JFH1 and Con1) was performed by PCR, detailed information is available on request. The reporter plasmid carrying the firefly luciferase (Fluc) gene under the control of the IFNβ promoter (pIFNβ-Luc) was provided by J. Jung (44). T. Fujita kindly provided FLAG-tagged expression vectors for RIG-I, RIG-I-N, TBK1, IKKε, IPS-1/MAVS and HA-IRF3-5D. The control pCMV-Renilla was from Promega.

Lentivector production and shRNA delivery

Overexpression of NAP1-EYFP and control EYFP was obtained by lentivector transduction on a pWPI backbone with blasticidin resistance (BLR) kindly provided by D. Trono. Lentiviral silencing vectors were derived from pLKO.1 TRC (Addgene). The control short-hairpin RNA (shRNA) was the pLKO.1 scramble from Addgene while for NAP1L1 targeting a specific targeting sequence was designed and cloned into pLKO.1 TRC (shNAP1L1) using the following oligonucleotides:

5'-ccggcctattctgaagcacttgaaactgcagtttcaagtgcttcagaataggtttttg -3' and

5'- ggataagacttcgtgaactttgacgtcaaagttcacgaagtcttatccaaaaacttaa -3'.

A LV for TLR3 reconstitution together with its GFP control was obtained from Sam Wilson (MRC – University of Glasgow Centre for Virus Research). Packaging in HEK 293T was performed according to standard procedures using the packaging plasmid psPAX2 and pMD2.G (Addgene). Cells' supernatants were filtered and kept at -80 °C in small aliquots until use.

In vitro transcription and electroporation of HCV SGR RNA

The HCV SGR constructs were linearized with XbaI and treated with mung-bean nuclease as described previously (79). RNA was transcribed in vitro from linearized constructs using the MEGAscript T7 kit (Ambion). Synthesized RNA was treated with DNase I and transfected into cells by electroporation.

PolyI:C (polyinosinic : polycytidylic acid sodium salt; Invivogen) was also transfected into cells by lipofection (Lipofectamine PLUS, Life Technologies) according to manufacturer's instructons.

Western-blotting, immunoprecipitation and immunofluorescence

Indirect immunofluorescence analysis (IF) and Western-blotting (WB) were performed essentially as previously described (80). Immunoprecipitation (IP) was performed by lysis of cells in RIPA buffer (50 mM Tris HCl pH7.5, 150 mM NaCl, 1% NP-40, 1% SDS, 1M PMSF, 1mM EDTA and proteinase inhibitors (cOmplete Mini, Roche). Lysates were cleared by centrifugation and incubated with anti-FLAG M2 agarose beads (Sigma-Aldrich), or with anti-NAP1L1 Ab/IgG control and protein A/G agarose beads, washed several

615 times in RIPA and eluted in SDS-PAGE sample buffer. The following
616 antibodies were used in this study: a sheep polyclonal against NS5A kindly
617 provided by M. Harris (1:200 IF; 1:2000 WB) (81); a rabbit polyclonal against
618 human NAP1L1 (Ab33076, Abcam) (1:200 IF; 1:1000 WB; 1:100 IP); a rabbit
619 polyclonal against human IRF3 kindly provided by T. Fujita (1:100 IF); a rabbit
620 monoclonal against human IRF3 (#4302 Cell Signaling) (1:500 WB); a rabbit
621 monoclonal against phosphorylated human IRF3 (#4947 Cell Signaling)
622 (1:500 WB); a rabbit monoclonal against human NF-κB p65/RELA (#8242 Cell
623 Signaling) (1:100 IF; 1:1000 WB); a rabbit monoclonal against phosphorylated
624 human NF-κB p65/RELA (#3033 Cell Signaling) (1:1000 WB); a mouse
625 monoclonal against human β-actin conjugated with peroxidase (A3854 Sigma-
626 Aldrich) (1:10000 WB); a mouse monoclonal against the FLAG tag (F1804
627 Sigma-Aldrich) (1:1000 WB); a mouse monoclonal against the HA tag
628 conjugated with peroxidase (H6533 Sigma-Aldrich) (1:10000 WB). Secondary
629 antibodies conjugated with AlexaFluor 488/594 were from Life Technologies
630 (1:500 IF) and peroxidase conjugates from Dako (1:5000 WB).
631
632 **Luciferase assay and real-time quantitative reverse transcription PCR**
633 Luciferase assays were conducted essentially as described previously (79,
634 80). For real-time quantitative reverse transcription PCR (qPCR) total cellular
635 RNA was extracted with the isol-RNA reagent (5 Prime) and treated with
636 DNAse I (Life Technologies). 500 ng were then reverse-transcribed with
637 random primers and M-MLV Reverse Transcriptase (Life Technologies).
638 Quantification of mRNA was obtained by real-time PCR using the Kapa Sybr
639 fast qPCR kit on a CFX96 Bio-Rad thermocycler. Primers for amplification are
640 available upon request.
641
642 **Transcriptome analysis by RNAseq**
643 Huh7-lunet cells were transduced with shNAP1L1 or shCTRL in triplicate and
644 incubated with puromicin for 3 days. Total RNA (Isol RNA lysis, Reagent 5
645 PRIME, Hamburg, DE) was extracted. Quality of extracted RNA was checked
646 by gel electrophoresis (ribosomal 18S and 28S), spectrophotometric analysis
647 (260/280>1.8) and Agilent bioanalyzer (RNA integrity number, RIN≥8). A

cDNA library of polyA-containing mRNA molecules was prepared (TruSeq, Illumina) and sequenced on the Illumina Platform (Hiseq2000 4-plex run, 50 bp reads, about 30M reads/sample) at IGA Technology Services (Udine, Italy). Raw data were subjected to quality control (FastQC) and mapped against the human genome RNA reference from NCBI using CLCbio sotware. The Bioconductor packages DESeq2 version 1.4.5 (82) and EdgeR (83) version 3.6.2 in the framework of R software version 3.1.0 were used to perform the differential gene expression analysis of mRNAseq data. Both the packages are based on the negative binomial distribution (NB) to model the gene reads counts and shrinkage estimator to estimate the per-gene NB dispersion parameters. Specifically, we used rounded gene counts as input and we estimated the per-gene NB dispersion parameter using the function DESeq for DESEQ2 while, for edgeR we used the function calcNormFactors with the default parameters. To detect outlier data after normalization we used the R packages arrayQualityMetrix (84) and before testing differential gene expression we dropped all genes with normalized counts below 14 to improve testing power while maintaining type I error rates. Estimated p-values for each gene were adjusted using the Benjamini-Hochberg method (85). Genes with adjusted $P<0.05$ and absolute Logarithmic base 2 fold change > 1 were selected. Data were finally analysed with the Ingenuity Pathway Analysis software. The significance values for the canonical pathway across the dataset shown in the Supplementary Table 1 are calculated by the Fisher's exact test right-tailed. The significance indicates the probability of association of molecules from our dataset with the canonical pathway by random chance alone.

Statistics

Three independent experiments in triplicate repeats were conducted for each condition examined, unless otherwise indicated in the figure legends. Mean values are shown with standard deviation and p-values, measured with a paired two-tailed t-test. Only significant p-values are indicated by the asterisks above the graphs ($p<0.01$ = ** highly significant; $p<0.05$ = * significant). Where asterisks are missing the differences are calculated as non-significant.

682 **Acknowledgments**

683 Work on flaviviruses in A.M.'s laboratory is supported by the Beneficientia
684 Stiftung. The funders had no role in study design, data collection and
685 interpretation, or the decision to submit the work for publication.

686

687 **References**

688 1. **Choo QL, Kuo G, Weiner AJ, Overby LR, Bradley DW, Houghton**
689 **M.** 1989. Isolation of a cDNA clone derived from a blood-borne non-A,
690 non-B viral hepatitis genome. Science **244:**359-362.
691 2. **Smith DB, Bukh J, Kuiken C, Muerhoff AS, Rice CM, Stapleton JT,**
692 **Simmonds P.** 2014. Expanded classification of hepatitis C virus into 7
693 genotypes and 67 subtypes: updated criteria and genotype assignment
694 web resource. Hepatology **59:**318-327.
695 3. **Miyanari Y, Atsuzawa K, Usuda N, Watashi K, Hishiki T, Zayas M,**
696 **Bartenschlager R, Wakita T, Hijikata M, Shimotohno K.** 2007. The
697 lipid droplet is an important organelle for hepatitis C virus production.
698 Nat Cell Biol **9:**1089-1097.
699 4. **Romero-Brey I, Merz A, Chiramel A, Lee JY, Chlanda P, Haselman**
700 **U, Santarella-Mellwig R, Habermann A, Hoppe S, Kallis S, Walther**
701 **P, Antony C, Krijnse-Locker J, Bartenschlager R.** 2013. Three-
702 dimensional architecture and biogenesis of membrane structures
703 associated with hepatitis C virus replication. PLoS Pathog **8:**e1003056.
704 5. **Boulant S, Targett-Adams P, McLauchlan J.** 2007. Disrupting the
705 association of hepatitis C virus core protein with lipid droplets
706 correlates with a loss in production of infectious virus. J Gen Virol
707 **88:**2204-2213.
708 6. **Masaki T, Suzuki R, Murakami K, Aizaki H, Ishii K, Murayama A,**
709 **Date T, Matsuura Y, Miyamura T, Wakita T, Suzuki T.** 2008.
710 Interaction of hepatitis C virus nonstructural protein 5A with core
711 protein is critical for the production of infectious virus particles. J Virol
712 **82:**7964-7976.
713 7. **Tellinghuisen TL, Foss KL, Treadaway J.** 2008. Regulation of
714 hepatitis C virion production via phosphorylation of the NS5A protein.
715 PLoS Pathog **4:**e1000032.

8. **Appel N, Zayas M, Miller S, Krijnse-Locker J, Schaller T, Friebe P, Kallis S, Engel U, Bartenschlager R.** 2008. Essential role of domain III of nonstructural protein 5A for hepatitis C virus infectious particle assembly. PLoS Pathog **4:**e1000035.
9. **Macdonald A, Harris M.** 2004. Hepatitis C virus NS5A: tales of a promiscuous protein. J Gen Virol **85:**2485-2502.
10. **Ross-Thriepland D, Harris M.** 2015. Hepatitis C virus NS5A: enigmatic but still promiscuous 10 years on! J Gen Virol **96:**727-738.
11. **IARC.** 2012. Hepatitits C virus. A review of human carcinogens Part B: Biological agents IARC Working Group on the Evaluation of Carcinogenic Risks to Humans**:**135-168.
12. **McGivern DR, Lemon SM.** 2011. Virus-specific mechanisms of carcinogenesis in hepatitis C virus associated liver cancer. Oncogene **30:**1969-1983.
13. **Lerat H, Honda M, Beard MR, Loesch K, Sun J, Yang Y, Okuda M, Gosert R, Xiao SY, Weinman SA, Lemon SM.** 2002. Steatosis and liver cancer in transgenic mice expressing the structural and nonstructural proteins of hepatitis C virus. Gastroenterology **122:**352-365.
14. **Wang AG, Lee DS, Moon HB, Kim JM, Cho KH, Choi SH, Ha HL, Han YH, Kim DG, Hwang SB, Yu DY.** 2009. Non-structural 5A protein of hepatitis C virus induces a range of liver pathology in transgenic mice. J Pathol **219:**253-262.
15. **Majumder M, Steele R, Ghosh AK, Zhou XY, Thornburg L, Ray R, Phillips NJ, Ray RB.** 2003. Expression of hepatitis C virus non-structural 5A protein in the liver of transgenic mice. FEBS Lett **555:**528-532.
16. **Gale M, Jr., Kwieciszewski B, Dossett M, Nakao H, Katze MG.** 1999. Antiapoptotic and oncogenic potentials of hepatitis C virus are linked to interferon resistance by viral repression of the PKR protein kinase. J Virol **73:**6506-6516.
17. **Ghosh AK, Steele R, Meyer K, Ray R, Ray RB.** 1999. Hepatitis C virus NS5A protein modulates cell cycle regulatory genes and promotes cell growth. J Gen Virol **80 (Pt 5):**1179-1183.

18. **Pichlmair A, Kandasamy K, Alvisi G, Mulhern O, Sacco R, Habjan M, Binder M, Stefanovic A, Eberle CA, Goncalves A, Burckstummer T, Muller AC, Fauster A, Holze C, Lindsten K, Goodbourn S, Kochs G, Weber F, Bartenschlager R, Bowie AG, Bennett KL, Colinge J, Superti-Furga G.** 2012. Viral immune modulators perturb the human molecular network by common and unique strategies. Nature **487:**486-490.

19. **de Chassey B, Navratil V, Tafforeau L, Hiet MS, Aublin-Gex A, Agaugue S, Meiffren G, Pradezynski F, Faria BF, Chantier T, Le Breton M, Pellet J, Davoust N, Mangeot PE, Chaboud A, Penin F, Jacob Y, Vidalain PO, Vidal M, Andre P, Rabourdin-Combe C, Lotteau V.** 2008. Hepatitis C virus infection protein network. Mol Syst Biol **4:**230.

20. **Chung HY, Gu M, Buehler E, MacDonald MR, Rice CM.** 2014. Seed sequence-matched controls reveal limitations of small interfering RNA knockdown in functional and structural studies of hepatitis C virus NS5A-MOBKL1B interaction. J Virol **88:**11022-11033.

21. **Ramage HR, Kumar GR, Verschueren E, Johnson JR, Von Dollen J, Johnson T, Newton B, Shah P, Horner J, Krogan NJ, Ott M.** 2015. A combined proteomics/genomics approach links hepatitis C virus infection with nonsense-mediated mRNA decay. Mol Cell **57:**329-340.

22. **Ishimi Y, Kikuchi A.** 1991. Identification and molecular cloning of yeast homolog of nucleosome assembly protein I which facilitates nucleosome assembly in vitro. J Biol Chem **266:**7025-7029.

23. **Park YJ, Luger K.** 2006. The structure of nucleosome assembly protein 1. Proc Natl Acad Sci U S A **103:**1248-1253.

24. **Park YJ, Luger K.** 2006. Structure and function of nucleosome assembly proteins. Biochem Cell Biol **84:**549-558.

25. **Loyola A, Almouzni G.** 2004. Histone chaperones, a supporting role in the limelight. Biochim Biophys Acta **1677:**3-11.

26. **Tyler JK.** 2002. Chromatin assembly. Cooperation between histone chaperones and ATP-dependent nucleosome remodeling machines. Eur J Biochem **269:**2268-2274.

27. **Asahara H, Tartare-Deckert S, Nakagawa T, Ikehara T, Hirose F, Hunter T, Ito T, Montminy M.** 2002. Dual roles of p300 in chromatin assembly and transcriptional activation in cooperation with nucleosome assembly protein 1 in vitro. Mol Cell Biol **22:**2974-2983.

28. **Rehtanz M, Schmidt HM, Warthorst U, Steger G.** 2004. Direct interaction between nucleosome assembly protein 1 and the papillomavirus E2 proteins involved in activation of transcription. Mol Cell Biol **24:**2153-2168.

29. **Sharma N, Nyborg JK.** 2008. The coactivators CBP/p300 and the histone chaperone NAP1 promote transcription-independent nucleosome eviction at the HTLV-1 promoter. Proc Natl Acad Sci U S A **105:**7959-7963.

30. **Vardabasso C, Manganaro L, Lusic M, Marcello A, Giacca M.** 2008. The histone chaperone protein Nucleosome Assembly Protein-1 (hNAP-1) binds HIV-1 Tat and promotes viral transcription. Retrovirology **5:**8.

31. **De Marco A, Dans PD, Knezevich A, Maiuri P, Pantano S, Marcello A.** 2010. Subcellular localization of the interaction between the human immunodeficiency virus transactivator Tat and the nucleosome assembly protein 1. Amino Acids **38:**1583-1593.

32. **Li Z, Gadue P, Chen K, Jiao Y, Tuteja G, Schug J, Li W, Kaestner KH.** 2012. Foxa2 and H2A.Z mediate nucleosome depletion during embryonic stem cell differentiation. Cell **151:**1608-1616.

33. **Gong H, Yan Y, Fang B, Xue Y, Yin P, Li L, Zhang G, Sun X, Chen Z, Ma H, Yang C, Ding Y, Yong Y, Zhu Y, Yang H, Komuro I, Ge J, Zou Y.** 2014. Knockdown of nucleosome assembly protein 1-like 1 induces mesoderm formation and cardiomyogenesis via notch signaling in murine-induced pluripotent stem cells. Stem Cells **32:**1759-1773.

34. **Nagata T, Takahashi Y, Ishii Y, Asai S, Nishida Y, Murata A, Koshinaga T, Fukuzawa M, Hamazaki M, Asami K, Ito E, Ikeda H, Takamatsu H, Koike K, Kikuta A, Kuroiwa M, Watanabe A, Kosaka Y, Fujita H, Miyake M, Mugishima H.** 2003. Transcriptional profiling in

817 hepatoblastomas using high-density oligonucleotide DNA array.
818 Cancer Genet Cytogenet **145:**152-160.
819 35. **Kidd M, Modlin IM, Mane SM, Camp RL, Eick G, Latich I.** 2006. The
820 role of genetic markers--NAP1L1, MAGE-D2, and MTA1--in defining
821 small-intestinal carcinoid neoplasia. Ann Surg Oncol **13:**253-262.
822 36. **Schimmack S, Taylor A, Lawrence B, Alaimo D, Schmitz-**
823 **Winnenthal H, Buchler MW, Modlin IM, Kidd M.** 2014. A mechanistic
824 role for the chromatin modulator, NAP1L1, in pancreatic
825 neuroendocrine neoplasm proliferation and metastases. Epigenetics
826 Chromatin **7:**15.
827 37. **Koutsoudakis G, Kaul A, Steinmann E, Kallis S, Lohmann V,**
828 **Pietschmann T, Bartenschlager R.** 2006. Characterization of the
829 early steps of hepatitis C virus infection by using luciferase reporter
830 viruses. J Virol **80:**5308-5320.
831 38. **Ohkuni K, Shirahige K, Kikuchi A.** 2003. Genome-wide expression
832 analysis of NAP1 in Saccharomyces cerevisiae. Biochem Biophys Res
833 Commun **306:**5-9.
834 39. **Horner SM, Gale M, Jr.** 2013. Regulation of hepatic innate immunity
835 by hepatitis C virus. Nat Med **19:**879-888.
836 40. **Chiang HS, Zhao Y, Song JH, Liu S, Wang N, Terhorst C, Sharpe**
837 **AH, Basavappa M, Jeffrey KL, Reinecker HC.** 2013. GEF-H1
838 controls microtubule-dependent sensing of nucleic acids for antiviral
839 host defenses. Nat Immunol **15:**63-71.
840 41. **Luna JM, Scheel TK, Danino T, Shaw KS, Mele A, Fak JJ,**
841 **Nishiuchi E, Takacs CN, Catanese MT, de Jong YP, Jacobson IM,**
842 **Rice CM, Darnell RB.** 2015. Hepatitis C virus RNA functionally
843 sequesters miR-122. Cell **160:**1099-1110.
844 42. **Sumpter R, Jr., Loo YM, Foy E, Li K, Yoneyama M, Fujita T, Lemon**
845 **SM, Gale M, Jr.** 2005. Regulating intracellular antiviral defense and
846 permissiveness to hepatitis C virus RNA replication through a cellular
847 RNA helicase, RIG-I. J Virol **79:**2689-2699.
848 43. **Miorin L, Albornoz A, Baba MM, D'Agaro P, Marcello A.** 2012.
849 Formation of membrane-defined compartments by tick-borne

encephalitis virus contributes to the early delay in interferon signaling. Virus Res **163:**660-666.

44. **Lin R, Genin P, Mamane Y, Hiscott J.** 2000. Selective DNA binding and association with the CREB binding protein coactivator contribute to differential activation of alpha/beta interferon genes by interferon regulatory factors 3 and 7. Mol Cell Biol **20:**6342-6353.

45. **Jaeckel E, Cornberg M, Wedemeyer H, Santantonio T, Mayer J, Zankel M, Pastore G, Dietrich M, Trautwein C, Manns MP, German Acute Hepatitis CTG.** 2001. Treatment of acute hepatitis C with interferon alfa-2b. N Engl J Med **345:**1452-1457.

46. **Sarasin-Filipowicz M, Oakeley EJ, Duong FH, Christen V, Terracciano L, Filipowicz W, Heim MH.** 2008. Interferon signaling and treatment outcome in chronic hepatitis C. Proc Natl Acad Sci U S A **105:**7034-7039.

47. **Chen L, Borozan I, Feld J, Sun J, Tannis LL, Coltescu C, Heathcote J, Edwards AM, McGilvray ID.** 2005. Hepatic gene expression discriminates responders and nonresponders in treatment of chronic hepatitis C viral infection. Gastroenterology **128:**1437-1444.

48. **Asselah T, Bieche I, Narguet S, Sabbagh A, Laurendeau I, Ripault MP, Boyer N, Martinot-Peignoux M, Valla D, Vidaud M, Marcellin P.** 2008. Liver gene expression signature to predict response to pegylated interferon plus ribavirin combination therapy in patients with chronic hepatitis C. Gut **57:**516-524.

49. **Dill MT, Duong FH, Vogt JE, Bibert S, Bochud PY, Terracciano L, Papassotiropoulos A, Roth V, Heim MH.** 2011. Interferon-induced gene expression is a stronger predictor of treatment response than IL28B genotype in patients with hepatitis C. Gastroenterology **140:**1021-1031.

50. **Bellecave P, Sarasin-Filipowicz M, Donze O, Kennel A, Gouttenoire J, Meylan E, Terracciano L, Tschopp J, Sarrazin C, Berg T, Moradpour D, Heim MH.** 2010. Cleavage of mitochondrial antiviral signaling protein in the liver of patients with chronic hepatitis C correlates with a reduced activation of the endogenous interferon system. Hepatology **51:**1127-1136.

884 51. **Li K, Li NL, Wei D, Pfeffer SR, Fan M, Pfeffer LM.** 2012. Activation of
885 chemokine and inflammatory cytokine response in hepatitis C virus-
886 infected hepatocytes depends on Toll-like receptor 3 sensing of
887 hepatitis C virus double-stranded RNA intermediates. Hepatology
888 **55:**666-675.
889 52. **Wang N, Liang Y, Devaraj S, Wang J, Lemon SM, Li K.** 2009. Toll-
890 like receptor 3 mediates establishment of an antiviral state against
891 hepatitis C virus in hepatoma cells. J Virol **83:**9824-9834.
892 53. **Arnaud N, Dabo S, Akazawa D, Fukasawa M, Shinkai-Ouchi F,**
893 **Hugon J, Wakita T, Meurs EF.** 2011. Hepatitis C virus reveals a novel
894 early control in acute immune response. PLoS Pathog **7:**e1002289.
895 54. **Kanazawa N, Kurosaki M, Sakamoto N, Enomoto N, Itsui Y,**
896 **Yamashiro T, Tanabe Y, Maekawa S, Nakagawa M, Chen CH,**
897 **Kakinuma S, Oshima S, Nakamura T, Kato T, Wakita T, Watanabe**
898 **M.** 2004. Regulation of hepatitis C virus replication by interferon
899 regulatory factor 1. J Virol **78:**9713-9720.
900 55. **Kumar A, Yang YL, Flati V, Der S, Kadereit S, Deb A, Haque J, Reis**
901 **L, Weissmann C, Williams BR.** 1997. Deficient cytokine signaling in
902 mouse embryo fibroblasts with a targeted deletion in the PKR gene:
903 role of IRF-1 and NF-kappaB. EMBO J **16:**406-416.
904 56. **McAllister CS, Samuel CE.** 2009. The RNA-activated protein kinase
905 enhances the induction of interferon-beta and apoptosis mediated by
906 cytoplasmic RNA sensors. J Biol Chem **284:**1644-1651.
907 57. **Foy E, Li K, Sumpter R, Jr., Loo YM, Johnson CL, Wang C, Fish**
908 **PM, Yoneyama M, Fujita T, Lemon SM, Gale M, Jr.** 2005. Control of
909 antiviral defenses through hepatitis C virus disruption of retinoic acid-
910 inducible gene-I signaling. Proc Natl Acad Sci U S A **102:**2986-2991.
911 58. **Foy E, Li K, Wang C, Sumpter R, Jr., Ikeda M, Lemon SM, Gale M,**
912 **Jr.** 2003. Regulation of interferon regulatory factor-3 by the hepatitis C
913 virus serine protease. Science **300:**1145-1148.
914 59. **Meylan E, Curran J, Hofmann K, Moradpour D, Binder M,**
915 **Bartenschlager R, Tschopp J.** 2005. Cardif is an adaptor protein in
916 the RIG-I antiviral pathway and is targeted by hepatitis C virus. Nature
917 **437:**1167-1172.

60. **Baril M, Racine ME, Penin F, Lamarre D.** 2009. MAVS dimer is a crucial signaling component of innate immunity and the target of hepatitis C virus NS3/4A protease. J Virol **83:**1299-1311.

61. **Li K, Foy E, Ferreon JC, Nakamura M, Ferreon AC, Ikeda M, Ray SC, Gale M, Jr., Lemon SM.** 2005. Immune evasion by hepatitis C virus NS3/4A protease-mediated cleavage of the Toll-like receptor 3 adaptor protein TRIF. Proc Natl Acad Sci U S A **102:**2992-2997.

62. **Lin R, Lacoste J, Nakhaei P, Sun Q, Yang L, Paz S, Wilkinson P, Julkunen I, Vitour D, Meurs E, Hiscott J.** 2006. Dissociation of a MAVS/IPS-1/VISA/Cardif-IKKepsilon molecular complex from the mitochondrial outer membrane by hepatitis C virus NS3-4A proteolytic cleavage. J Virol **80:**6072-6083.

63. **Yang Y, Liang Y, Qu L, Chen Z, Yi M, Li K, Lemon SM.** 2007. Disruption of innate immunity due to mitochondrial targeting of a picornaviral protease precursor. Proc Natl Acad Sci U S A **104:**7253-7258.

64. **Gale MJ, Jr., Korth MJ, Tang NM, Tan SL, Hopkins DA, Dever TE, Polyak SJ, Gretch DR, Katze MG.** 1997. Evidence that hepatitis C virus resistance to interferon is mediated through repression of the PKR protein kinase by the nonstructural 5A protein. Virology **230:**217-227.

65. **Taylor DR, Shi ST, Romano PR, Barber GN, Lai MM.** 1999. Inhibition of the interferon-inducible protein kinase PKR by HCV E2 protein. Science **285:**107-110.

66. **Noguchi T, Satoh S, Noshi T, Hatada E, Fukuda R, Kawai A, Ikeda S, Hijikata M, Shimotohno K.** 2001. Effects of mutation in hepatitis C virus nonstructural protein 5A on interferon resistance mediated by inhibition of PKR kinase activity in mammalian cells. Microbiol Immunol **45:**829-840.

67. **Kaukinen P, Sillanpaa M, Nousiainen L, Melen K, Julkunen I.** 2013. Hepatitis C virus NS2 protease inhibits host cell antiviral response by inhibiting IKKepsilon and TBK1 functions. J Med Virol **85:**71-82.

68. **Goonawardane N, Gebhardt A, Bartlett C, Pichlmair A, Harris M.** 2017. Phosphorylation of serine 225 in hepatitis C virus NS5A regulates protein-protein interactions. J Virol doi:10.1128/JVI.00805-17.
69. **Verbruggen P, Ruf M, Blakqori G, Overby AK, Heidemann M, Eick D, Weber F.** 2011. Interferon antagonist NSs of La Crosse virus triggers a DNA damage response-like degradation of transcribing RNA polymerase II. J Biol Chem **286:**3681-3692.
70. **Le May N, Dubaele S, Proietti De Santis L, Billecocq A, Bouloy M, Egly JM.** 2004. TFIIH transcription factor, a target for the Rift Valley hemorrhagic fever virus. Cell **116:**541-550.
71. **Le May N, Mansuroglu Z, Leger P, Josse T, Blot G, Billecocq A, Flick R, Jacob Y, Bonnefoy E, Bouloy M.** 2008. A SAP30 complex inhibits IFN-beta expression in Rift Valley fever virus infected cells. PLoS Pathog **4:**e13.
72. **Thomas D, Blakqori G, Wagner V, Banholzer M, Kessler N, Elliott RM, Haller O, Weber F.** 2004. Inhibition of RNA polymerase II phosphorylation by a viral interferon antagonist. J Biol Chem **279:**31471-31477.
73. **Marazzi I, Ho JS, Kim J, Manicassamy B, Dewell S, Albrecht RA, Seibert CW, Schaefer U, Jeffrey KL, Prinjha RK, Lee K, Garcia-Sastre A, Roeder RG, Tarakhovsky A.** 2012. Suppression of the antiviral response by an influenza histone mimic. Nature **483:**428-433.
74. **Friebe P, Boudet J, Simorre JP, Bartenschlager R.** 2005. Kissing-loop interaction in the 3' end of the hepatitis C virus genome essential for RNA replication. J Virol **79:**380-392.
75. **Hope RG, McLauchlan J.** 2000. Sequence motifs required for lipid droplet association and protein stability are unique to the hepatitis C virus core protein. J Gen Virol **81:**1913-1925.
76. **Lindenbach BD, Evans MJ, Syder AJ, Wolk B, Tellinghuisen TL, Liu CC, Maruyama T, Hynes RO, Burton DR, McKeating JA, Rice CM.** 2005. Complete replication of hepatitis C virus in cell culture. Science **309:**623-626.
77. **Wakita T, Pietschmann T, Kato T, Date T, Miyamoto M, Zhao Z, Murthy K, Habermann A, Krausslich HG, Mizokami M,**

Bartenschlager R, Liang TJ. 2005. Production of infectious hepatitis C virus in tissue culture from a cloned viral genome. Nat Med **11:**791-796.

78. **Targett-Adams P, McLauchlan J.** 2005. Development and characterization of a transient-replication assay for the genotype 2a hepatitis C virus subgenomic replicon. J Gen Virol **86:**3075-3080.

79. **Bartolomei G, Cevik RE, Marcello A.** 2011. Modulation of hepatitis C virus replication by iron and hepcidin in Huh7 hepatocytes. J Gen Virol **92:**2072-2081.

80. **Albornoz A, Carletti T, Corazza G, Marcello A.** 2014. The Stress Granule Component TIA-1 Binds Tick-Borne Encephalitis Virus RNA and Is Recruited to Perinuclear Sites of Viral Replication To Inhibit Viral Translation. J Virol **88:**6611-6622.

81. **Macdonald A, Crowder K, Street A, McCormick C, Saksela K, Harris M.** 2003. The hepatitis C virus non-structural NS5A protein inhibits activating protein-1 function by perturbing ras-ERK pathway signaling. J Biol Chem **278:**17775-17784.

82. **Love MI, Huber W, Anders S.** 2014. Moderated estimation of fold change and dispersion for RNA-seq data with DESeq2. Genome Biol **15:**550.

83. **McCarthy DJ, Smyth GK.** 2009. Testing significance relative to a fold-change threshold is a TREAT. Bioinformatics **25:**765-771.

84. **Kauffmann A, Gentleman R, Huber W.** 2009. arrayQualityMetrics--a bioconductor package for quality assessment of microarray data. Bioinformatics **25:**415-416.

85. **Benjamini Y, Hochberg Y.** 1995. Controlling the false discovery rate: a practical and powerful approach to multiple testing. Journal of the Royal Statistical Society, Series B **57:**289-300.

Figure Legends

Figure 1 – HCV NS5A binds NAP1L1.

A) Co-immune precipitation of flag-tagged NS5A and HA-NAP1L1 in HEK 293T cells. Transfected cells were lysed, co-IP with anti-FLAG agarose beads and blotted against α-FLAG or α-HA antibodies as indicated. A plasmid encoding for HIV-1 flag-tagged Tat was used as positive control.

B) NS5A interacts with endogenous NAP1L1 during HCV replication. Huh7-Lunet cells were electroporated with sub-genomic SGR-JFH1/Luc or mock transfected. At 72 hpe cell lysates were incubated with α-NAP1L1 antibodies or with matching irrelevant IgGs. Input and co-IP samples were then immuno-blotted with α-NAP1L1 and α-NS5A antibodies as indicated (IgH, Immunoglobulin heavy-chain).

C) NS5A and NAP1L1 co-localize during HCV replication. Huh7-Lunet cells were either mock electroporated or treated with the sub-genomic HCV replicon SGR-JFH1/Luc or with SGR-FK-Luc-JFH1/ΔE1-E2 and fixed at 72 hpe. Indirect immunofluorescence analysis was performed with α-NAP1L1 (green) and α-NS5A (red) antibodies and corresponding fluorescent secondary antibodies (scale bar 10 μm). Colocalization is shown in the merge channel (Pearson's correlation coefficient of 0.658 for SGR-JFH1/Luc and 0.731 for SGR-FK-Luc-JFH1/ΔE1-E2). The inset shows a high magnification image. Diffused, cytoplasmic localization of NAP1L1 in mock cells is also shown for comparison (above).

Figure 2 – HCV JFH1 NS5A targets NAP1L1 for proteasome-mediated degradation.

A) HCV NS5A from Con1 and H77 interact with NAP1L1. HEK293T cells were transfected with flag-tagged NS5A from HCV genotypes as indicated. Transfected cells were lysed, co-IP with α -FLAG agarose beads and blotted against α-FLAG or α-HA antibodies.

B) HCV NS5A from JFH1 degrades NAP1L1. 293T cells were transfected with equal amount of HA-NAP1L1 (5 μg) and increasing amount of flag tagged NS5A from JFH1 or from Con1 (0, 2.5, 5 and 10 μg). After 24 hours cell lysates were immunoblotted with α-FLAG, α-HA, and α-Actin antibodies.

C) HCV NS5A-mediated degradation is proteasome dependent. HEK293T cells were co-transfected with HA-NAP1L1 and flag-NS5A, treated with the MG132 (5μM) for 14 h, and lysed. Samples were run and immunoblotted with α-HA, α-FLAG and α-Actin antibodies.

D) HCV replication induces NAP1L1 degradation. Huh7-Lunet cells were electroporated with SGR-JFH1/Luc RNA or mock transfected. Cells were treated with 200 μM Cycloheximide (CHX) for 1 and 3 hours and lysed. Samples were run and immunoblotted with α-HA, α-FLAG and α-Actin antibodies.

E) CLUSTAL O (1.2.4) multiple sequence alignment NS5A from different HCV genotypes. The asterisk character (*) indicates all the sequences that share the same amino acid. Gaps are indicated by the minus character (-). The cluster of Serines implcated in NS5A binding are boxed.

Figure 3 – NAP1L1 interacts with the extreme carboxy-terminus of NS5A.

A) Diagram of NS5A and mutants produced in this work. The full-length of JFH1 NS5A is shown with the flag-tag at the N-terminus, the amphipathic helix (AH) for membrane tethering, domains I, II and III with the low-complexity sequences (LCS) I and II. AH-fused domain III (AH-D3-FL) is deleted from the C-terminus in 6 fragments (AH-D3.1-6). The amino acid sequence of the C-terminal region of NS5A encompassing S452/454/457A (Serines are in bold) is also shown, together with the sequences of the deletion mutant NS5A-delB and the triple S>A mutant NS5A-m2.

B) NAP1L1 binds Domain III of NS5A. HEK293T cells were transfected with the indicated domains fused to AH together with HA-NAP1L1. Transfected cells were lysed, co-IP with anti-FLAG agarose beads and blotted against α-FLAG or α-HA antibodies. White asterisks (*) indicate the position of the NS5A mutants that are distinguishable from the heavy (IgH) and light (IgL) immunoglobulin chains.

C) NAP1L1 binds the extreme C-terminus of NS5A. HEK293T cells were transfected with expression plasmids encoding for NS5A Domain III fused to AH carrying progressive deletions from the C-terminus as indicated in the diagram (Figure 3A). Co-IP was conducted as in Figure 3B.

D) NS5A mutants delB and m2 do not bind NAP1L1. HEK293T were

transfected with expression plasmids for NS5A mutants delB and m2 described in Figure 3A. Co-IP was conducted as in Figure 3B.

E) NS5A mutants delB and m2 lose colocalization with NS5A. Huh7-Lunet cells were electroporated with SGR-JFH1/Luc and with mutants SGR-JFH1/Luc_m2 and SGR-JFH1/Luc_delB and fixed at 72 hpe. Indirect immunofluorescence analysis was performed with α-NAP1L1 (green) and α-NS5A (red) antibodies and corresponding fluorescent secondary antibodies (scale bar 10 μm). Colocalization is shown in the merge channel.

Figure 4 – HCV does not require NAP1L1 for replication and infectivity

A) NS5A and NAP1L1-EYFP co-localize during HCV replication. Huh7-Lunet cells were transduced with a lentiviral vector (LV) expressing NAP1L1-EYFP and then either mock electroporated or treated with the sub-genomic HCV replicon SGR-JFH1/Luc and fixed at 72 hpe. Indirect immunofluorescence analysis was performed with α-NS5A (red) (scale bar 10 μm).

B) NAP1L1 overexpression does not affect HCV genome replication. Huh7-Lunet cells were transduced with a lentiviral vector (LV) expressing EYFP or NAP1L1-EYFP at an efficiency >85% on average as measured by cytofluorimetric analysis. Cells were then electroporated with the HCV SGR JFH1/Luc RNA and luciferase monitored at the indicated time points. Values are normalized to the luciferase signal at 4 hours post-electroporation. Average of 3 independent replicates are shown with standard deviations.

C) Depletion of NAP1L1 by shRNA. Huh7-Lunet cells were transduced with LV expressing shRNA targeting NAP1L1 (shNAP1L1) or non-targeting control (shCTRL). After selection with puromycin, cells were electroporated with HCV SGR JFH1/Luc RNA and protein levels detected by WB.

D) Depletion of NAP1L1 does not affect HCV genome replication. Huh7-Lunet cells were treated as in Figure 4C and the luciferase signal measured as in Figure 4B.

E) Depletion of NAP1L1 does not affect HCV infectivity. Huh7-Lunet cells treated with shRNAs as in Figure 4C were electroporated with full-length HCV JFH1 RNA. At the indicated time points, the supernatant was collected and used to infect naïve Huh7.5 cells at various dilutions. The 50% tissue culture infectious dose (TCID50) was then calculated counting cells stained with the

NS5A antiserum.

F) Mutagenesis of the NAP1L1 binding site of NS5A does not affect HCV genome replication. Huh7-Lunet cells were electroporated with HCV SGR JFH1/Luc RNA from wt, the m2 mutant of NS5A or the GND mutant of NS5B, which is replication defective. Luciferase was measured as in Figure 4B.

Figure 5 – The interaction with HCV NS5A inhibits NAP1L1 nuclear translocation.

A) SGR-JFH1 NS5A inhibits NAP1L1 nuclear localization. Huh7-Lunet cells were electroporated with HCV SGR-JFH1/Luc RNA or the mutant replicon SGR-JFH1/m2 or control SGR-JFH1/GND as indicated. At 63 h.p.e., cells were treated with 150 nM LMB for 9 hours. Cells were then fixed and stained for NS5A and NAP1L1. Scale bar = 10 μm.

B) Quantification of SGR-JFH1 NS5A inhibition of NAP1L1 nuclear localization. 300 cells treated as in Figure 5A were visually scored for NAP1L1 nuclear localization in the presence of NS5A. The investigator was blinded to the group allocation during visual counting. Average of 3 independent replicates are shown with standard deviations.

C) Con1 NS5A mutant m2 does not bind NAP1L1. HEK293T were transfected with expression plasmids for Con1 NS5A and m2. Co-IP was conducted as in Figure 3B.

D) Both JFH1 and Con1-derived NS5A inhibit nuclear translocation of NAP1L1. Huh7-Lunet cells were transfected with expression plasmids for NS5A from JFH1 or Con1 and their respective m2 mutants. Cells were treated with LMB as described above, fixed and stained for ectopic flag-tagged NS5A and endogenous NAP1L1. Scale bar = 10 μm.

E) Quantification of NS5A inhibition of NAP1L1 nuclear localization. Cells treated as in Figure 5C were visually scored as described above (Figure 5B).

Figure 6 – NAP1L1 is involved in the innate immunity response.

A) Whole-genome transcriptome analysis in NAP1L1-depleted cells. Huh7-Lunet cells were treated with shNAP1L1/shCTRL followed by RNAseq analysis. Black bars show the levels of 15 down-regulated genes (fold change ≤ -2) and 2 up-regulated genes (fold change ≥ 2), which were further validated

by qRT-PCR (grey bars) normalized for β-actin.

B) Induction of ISG genes is not NAP1L1-dependent. Huh7-Lunet cells were treated with 1000 U/ml of IFNα for 8 hours. UBD, GBP2, IFITM3 and GAPDH mRNA was measured by qRT-PCR normalized for β-actin in triplicate independent experiments. Shown are fold changes over basal, non induced levels ± SD.

C) IFN induction following poly(I:C) transfection in different cell lines. U2OS, Huh7-lunet and Huh7.5 were were transfected with 1 µg poly(I:C) for 8 hours. IFNβ mRNA levels were measured by qRT-PCR, normalized for β-actin and plotted against mock (lipofectamine). Average of 3 independent replicates are shown with standard deviations.

D) NAP1L1 depletion affects the induction of IFNβ mRNA by poly(I:C). U2OS cells treated with shNAP1L1/shCTRL for 3 days were transfected with 1 µg poly(I:C) for 8 hours. IFNβ mRNA levels were measured as above.

E) NAP1L1 depletion affects the induction of IFNβ by poly(I:C). U2OS cells were treated as above (Figure 6C). Secreted IFNβ protein was measured by a commercial ELISA in triplicate, quantified against a standard curve and plotted.

Figure 7 – NAP1L1 controls RELA levels and IRF3 activation.

A) NAP1L1 depletion affects RELA levels and IRF3 phosphorylation. U2OS cells were transduced with LV for shNAP1L1 or shCTRL and subsequently transfected with 1 µg poly(I:C) using lipofectamine (lipo). Protein levels as indicated were monitored by WB at 1-2-4 hours post transfection of poly(I:C).

B) NAP1L1 depletion decreases RELA protein levels. Blots as in Figure 7A were quantified to measure RELA and IRF3 protein levels using ImageJ. Shown is the ratio shNAP1L1/shCTRL in cells not transfected with poly(I:C). Average of 3 independent replicates are shown with standard deviations.

C) NAP1L1 depletion affects IRF3 phosphorylation. Blots as in Figure 7A were quantified to measure RELA and IRF3 phosphorylation levels using ImageJ. Shown is the ration phosphorylated/total protein in cells transfected with poly(I:C). Average of 3 independent replicates are shown with standard deviations.

D) NAP1L1 depletion reduces RELA nuclear translocation. U2OS cells were

transduced with LV for shNAP1L1 or shCTRL and subsequently transfected with 1 µg poly(I:C) for 8 hours. Cells were then fixed and stained for RELA.
E) NAP1L1 depletion reduces RELA nuclear translocation. Around 500 cells from the experiment shown in Figure 7D were counted for each condition to calculate the percentage of RELA nuclear translocation. Average of 3 independent replicates are shown with standard deviations.
F) NAP1L1 depletion reduces IRF3 nuclear translocation. U2OS cells were transduced with LV for shNAP1L1 or shCTRL and subsequently transfected with 1 µg poly(I:C) for 8 hours. Cells were then fixed and stained for IRF3.
G) NAP1L1 depletion reduces IRF3 nuclear translocation. Around 500 cells from the experiment shown in Figure 7F were counted for each condition to calculate the percentage of IRF3 nuclear translocation. Average of 3 independent replicates are shown with standard deviations.
H) HCV NS5A inhibits TBK1-mediated activation of IFNβ. HEK 293T cells were transfected with expression vectors for FLAG-tagged TBK1, NS5A or the mutants NS5A-m2 together with a reporter plasmid carrying the firefly luciferase (Fluc) gene under the control of the IFNβ promoter (pIFNβ-Luc) and the control pCMV-Renilla. Relative light units (RLUs) of luciferase activity was measured in quintuplicate independent experiments, normalized for Renilla, and represented as fold change over mock ± SD.

Figure 8 – NAP1L1 controls IRF3 phosphorylation at the TBK1/IKKε level.

A) Schematic representation of the RIG-I and TLR3 pathways. Both lead to activation of NF-κB and phosphorylation of IRF3 through MAVS/TBK1/IKKe or TRIF, respectively. NF-κB and pIRF3 translocate to the nucleus and activate IFNβ and other ISGs.
B) NAP1L1 does not affect constitutive IRF3-5D activity. Huh7-Lunet cells were transduced with LV for shNAP1L1 or shCTRL and subsequently transfected with an expression vector for IRF3-5D, the reporter IFNβ-Luc and the Renilla control. Cell lysates were blotted as indicated.
C) NAP1L1 does not affect constitutive IRF3-5D activity. Luciferase activity of cells from the experiment shown in Figure 7H was measured in triplicate independent experiments, normalized for Renilla. Average values are shown

with standard deviations.
D) Depletion of NAP1L1 affects TBK1/IKKε-mediated activation of IFNβ. HEK 293T cells were transduced with LV for shNAP1L1 or shCTRL and subsequently transfected with expression vectors for FLAG-tagged RIG-I, IPS-1/MAVS, TBK1 and IKKε together with the reporter IFNβ-Luc and the Renilla control. Cell lysates were blotted with anti-FLAG as indicated. Luciferase activity was measured in triplicate independent experiments, normalized for Renilla, and represented as fold change over mock ± SD.

Figure 9 – NAP1L1 controls the TLR3 pathway.
A) Depletion of NAP1L1 affects TRIF-mediated activation of IFNβ. Huh7-Lunet cells were transduced with LV for shNAP1L1 or shCTRL and subsequently transfected with expression vectors for TRIF together with the reporter IFNβ-Luc and the Renilla control. Luciferase activity was measured in triplicate independent experiments, normalized for Renilla, and represented as fold change over mock ± SD.
B) Depletion of NAP1L1 by LV shRNA treatment. Huh7-Lunet cells were transduced with LV for shNAP1L1 or shCTRL and then with LV expressing TLR3 or EGFP as control. 50 μg of Poly(I:C) was added to the medium for 24 hours. IFNβ mRNA levels for NAP1L1 were measured by qRT-PCR, normalized for β-actin and plotted against mock. Average of 3 independent replicates are shown with standard deviations.
C) Reconstitution of the TLR3 pathway. Cells were processed and TLR3 mRNA quantified as in Figure 9B above.
D) Depletion of NAP1L1 affects TLR3 signaling. Cells were processed and IFIT1 mRNA quantified as in Figure 9B above.

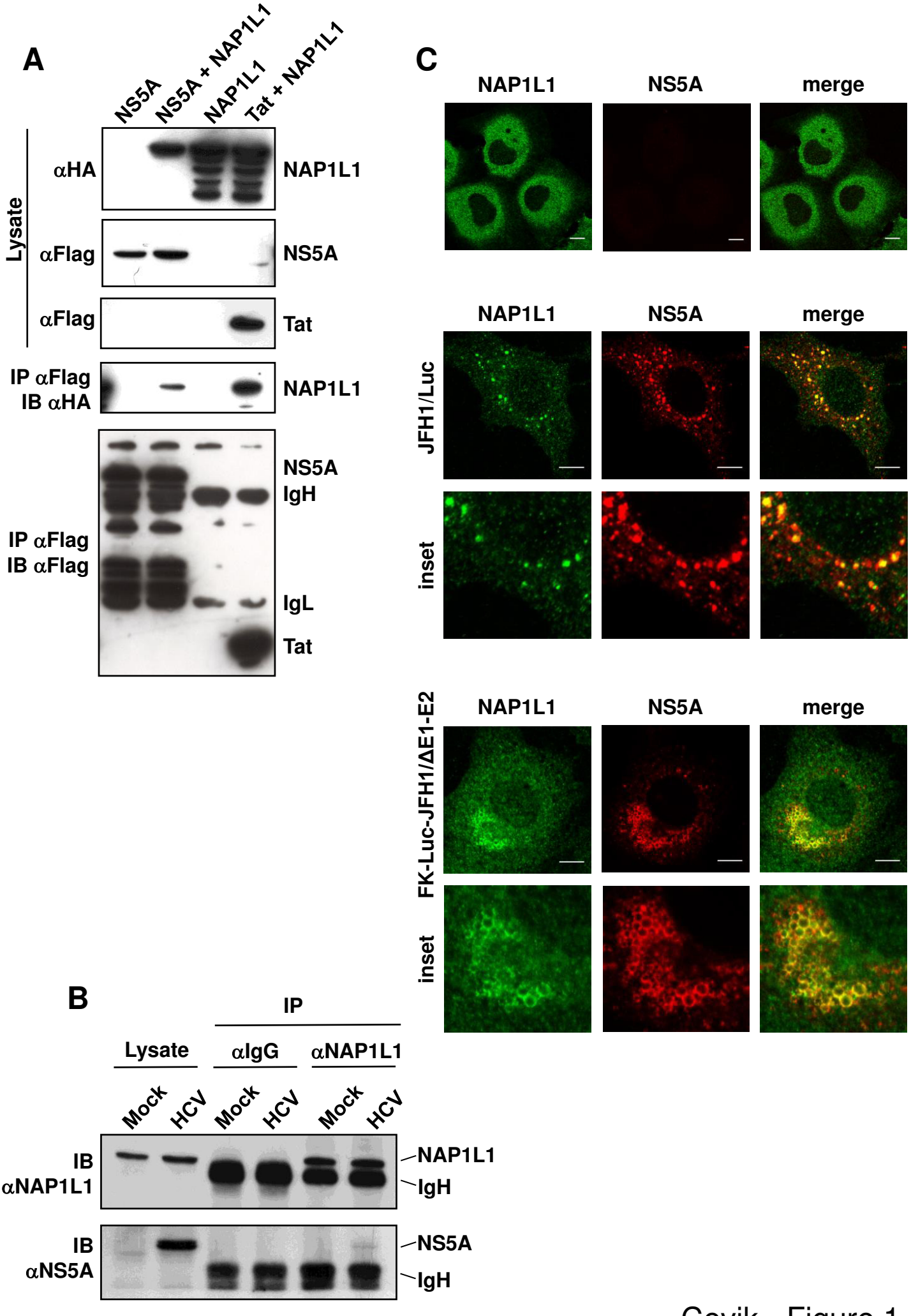

Cevik - Figure 1

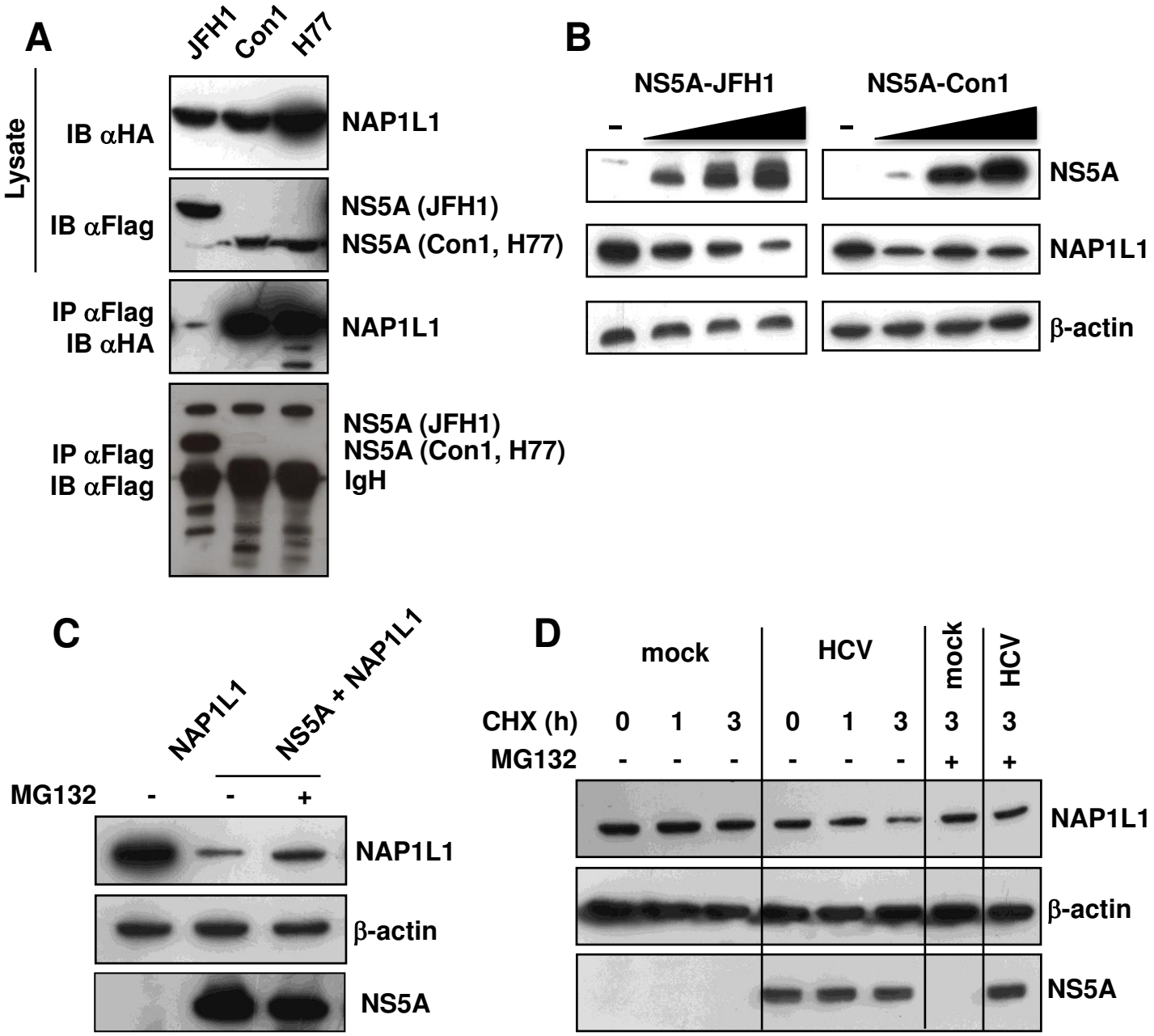

E

```
JFH-1 GSASSMPPLEGEPGDPDLESDQVELQPPPQGGGVAPGSGSGSWSTCSEED--DTTVCC
Con1  ESYSSMPPLEGEPGDPDLS-------------------DGSWSTVSEEA-SEDVVCC
H77   ESYSSMPPLEGEPGDPDLS-------------------DGSWSTVSSGADTEDVVCC
gt3   ESCSSMPPLEGEPGDPDLS-------------------CDSWSTVSDSE-EQSVVCC
gt4   GSYSSMPPLEGEPGDPDLT-------------------SDSWSTVSGS---EDVVCC
gt5   ASYSSMPPLEGEPGDPDLS-------------------SGSWSTVSGE---DNVVCC
gt6   GSFSSMPPLEGEPGDPDLS-------------------TGSWSTVSEE---DDVVCC
gt7   ISFSSMPPLEGEPGDPDLS-------------------DGSWSTVSTR---SDVICC
       * ***************                      ****  *          **
```

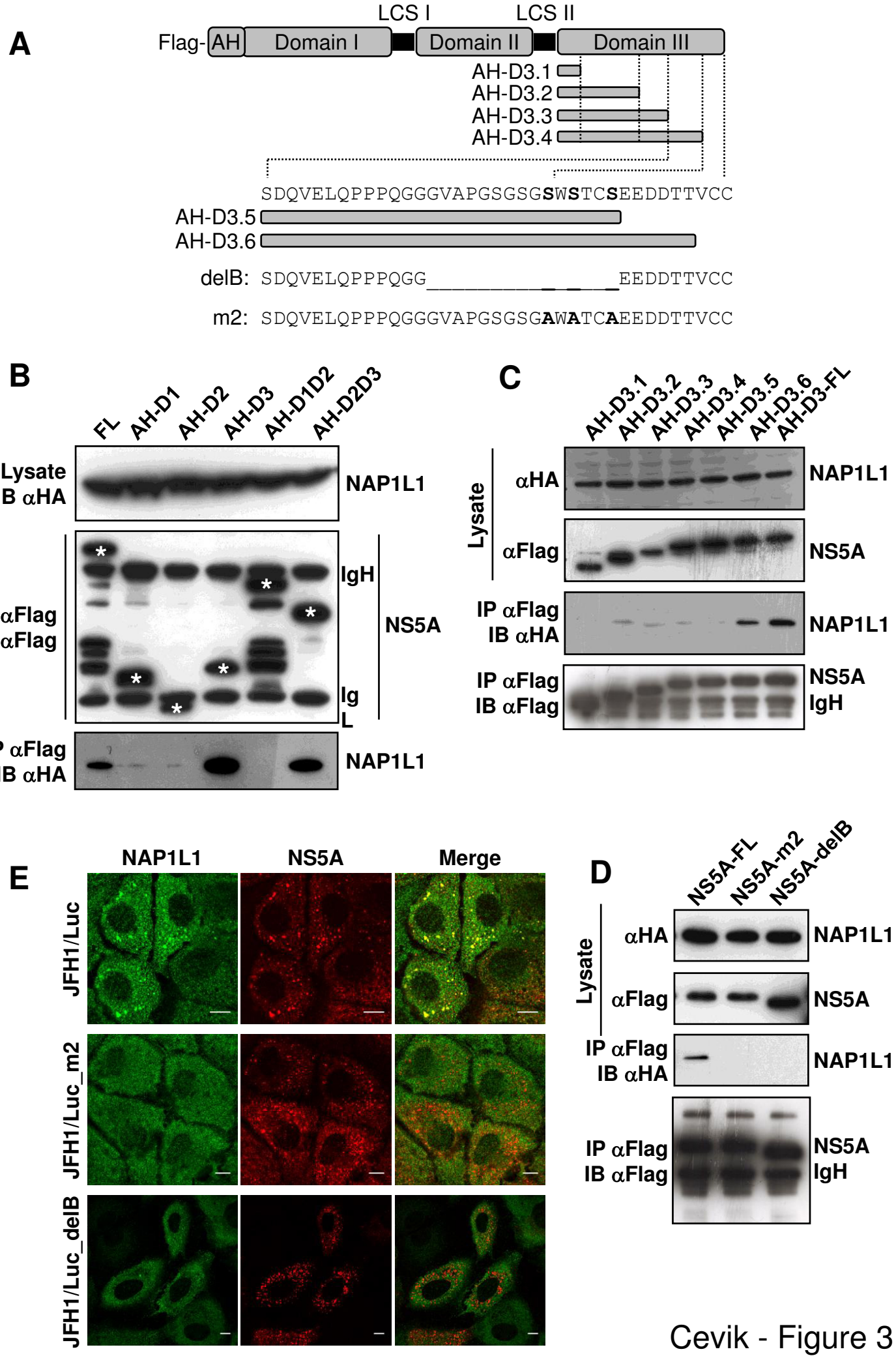

Cevik - Figure 3

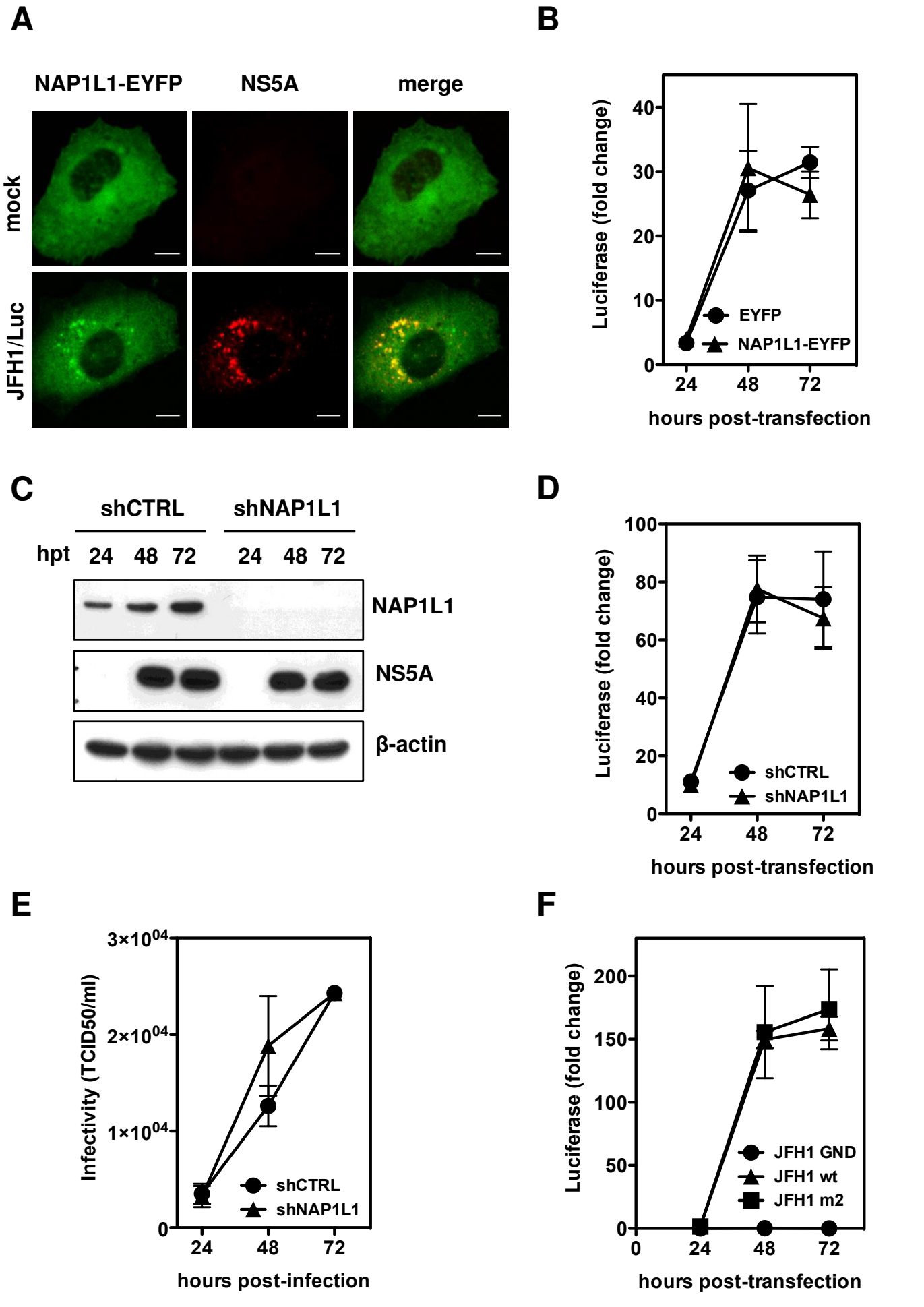

Cevik – Figure 4

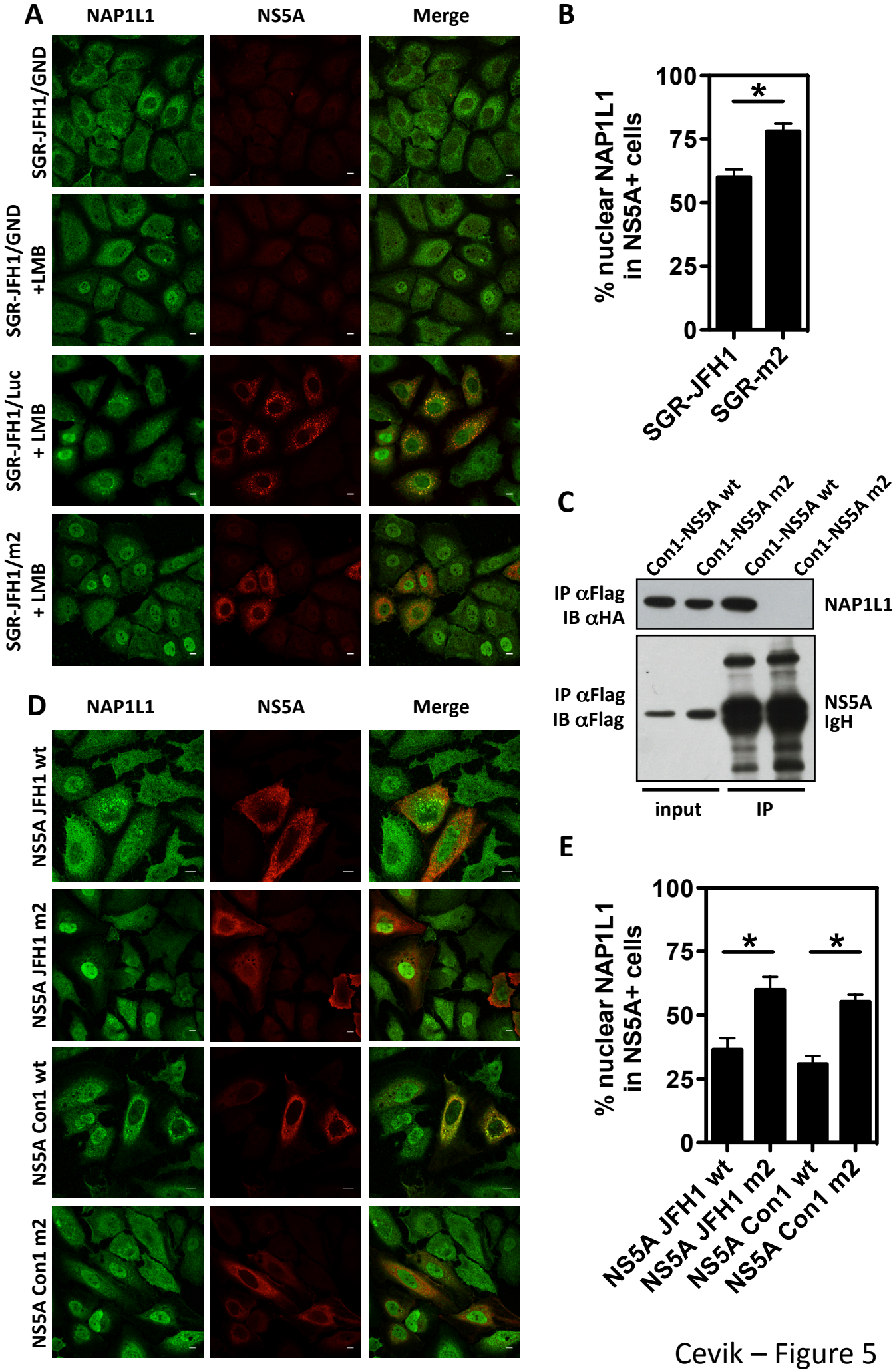

Cevik – Figure 5

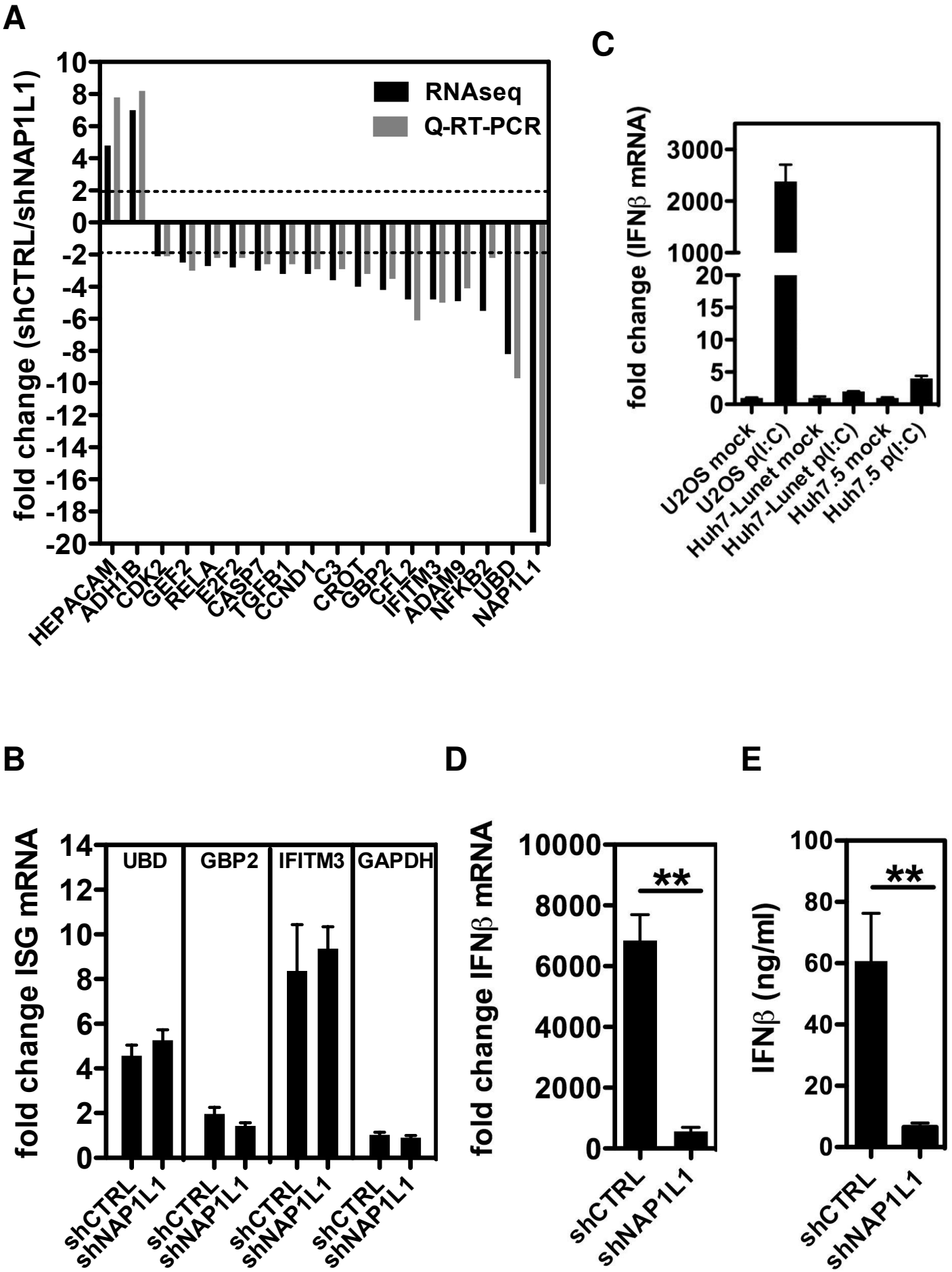

Cevik – Figure 6

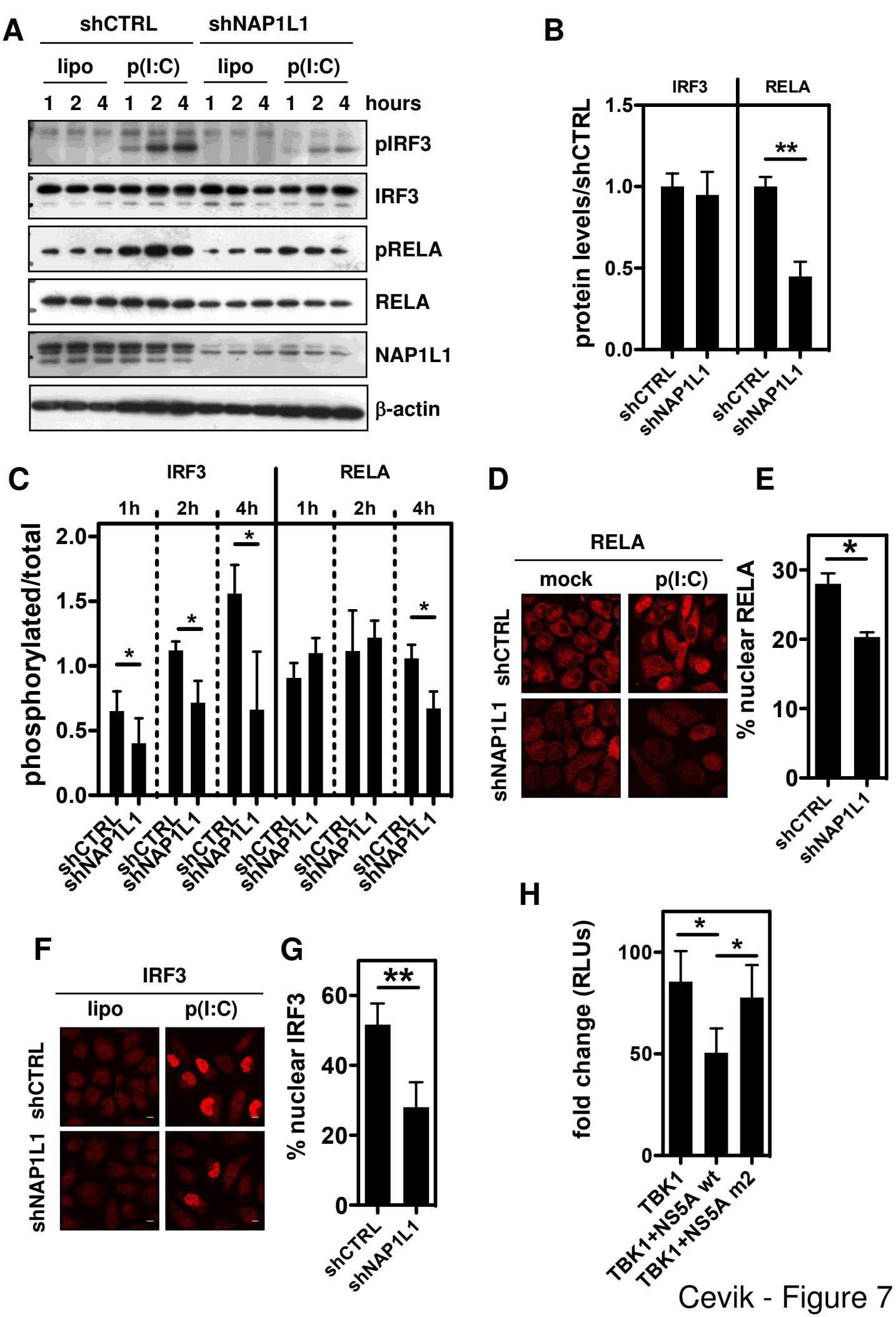

Cevik - Figure 7

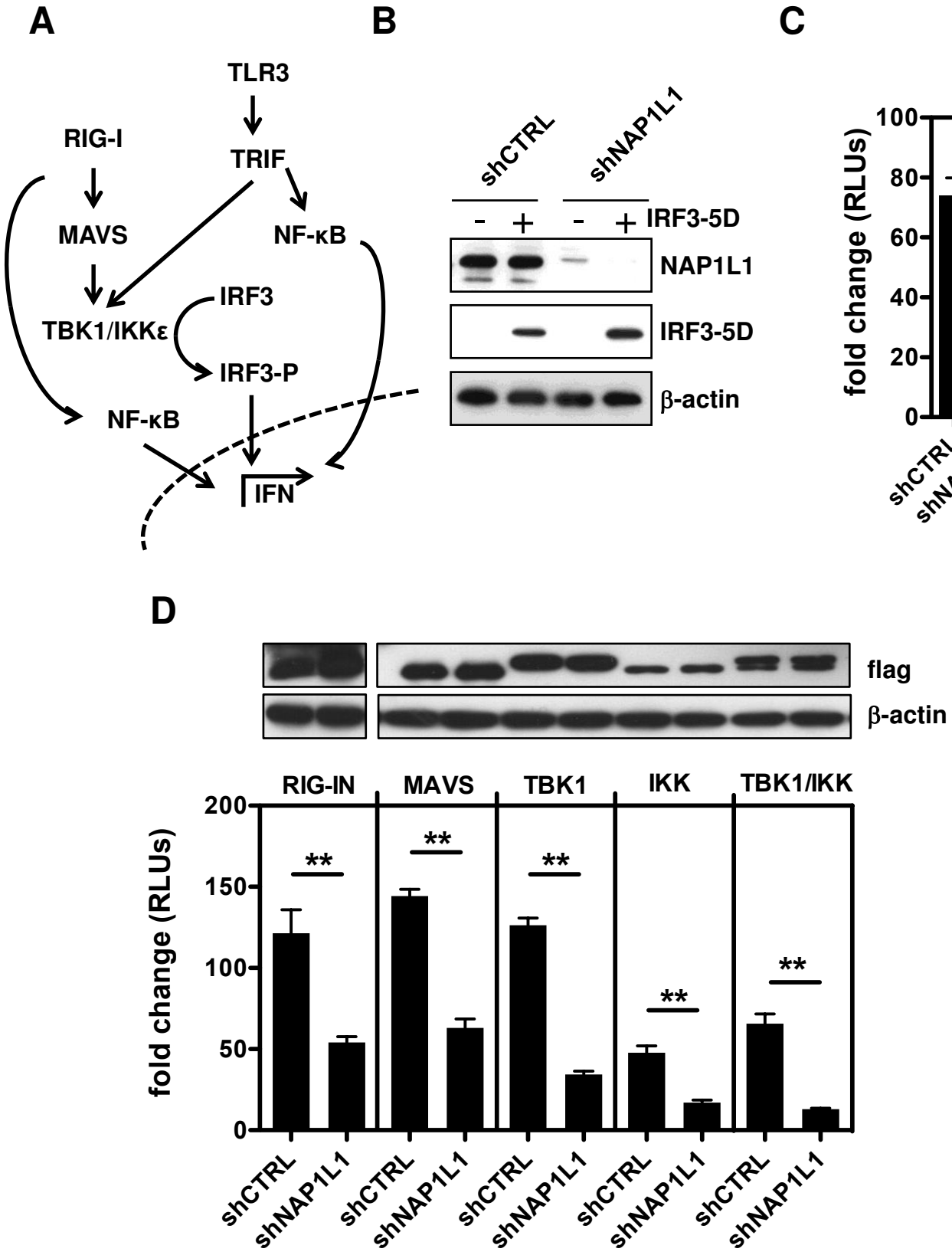

Cevik - Figure 8

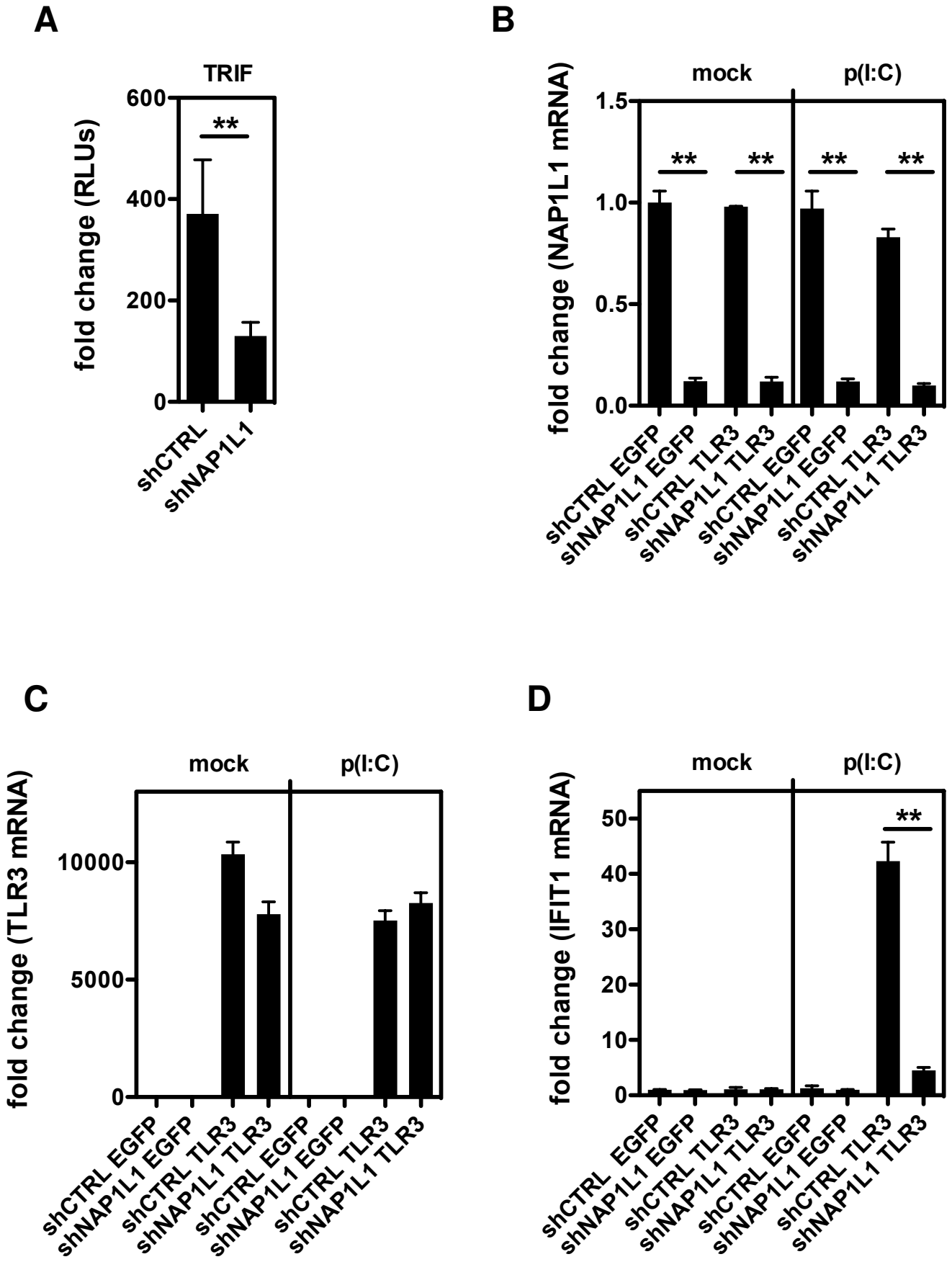

Cevik - Figure 9